MINE WASTE FAILURE: AN ANALYSIS OF EMPIRICAL AND GRAPHICAL RUNOUT PREDICTION METHODS

by

Gabriel Srour

A THESIS SUBMITTED IN PARTIAL FULFILLMENT OF

THE REQUIREMENTS FOR THE DEGREE OF

BACHELOR OF APPLIED SCIENCE

In

THE FACULTY OF APPLIED SCIENCE

(Geological Engineering)

This thesis conforms to the required standard

……………………………………………………………………

Supervisor: Scott McDougall

THE UNIVERSITY OF BRITISH COLUMBIA

(Vancouver)

April 2011

© Gabriel Srour, 2011

ABSTRACT

Historically, solid mine waste failures have taken many lives, destroyed many homes and have had many other negative impacts on the public and on mining companies. Laws passed after the 1966 Aberfan tragedy, which resulted in a loss of 144 lives, forced mining companies to reduce the risk involved in mine waste practice by making it illegal for mine waste dumps to fail. Since then, there have still been several failures, but mine waste management practices have improved. Recent efforts have focused on determining the risk involved with mine waste dumps. One approach to determining the risk associated with a mine waste dump is to predict the travel distance of a potential failure. The dilemma with runout prediction is that current runout prediction tools are often oversimplified, underdeveloped and under-tested.

This report provides the engineer with important background information into the construction, stability and risk involved with mine waste failures. It presents seven tools used to assess this risk and it further tests the accuracy of the tools on newly gathered data.

One empirical prediction tool proposed by Corominas (1996) was accurate within 7% and recorded a standard variation of 37% with respect to the observed tangent of the fahrböschung. Another formula developed by Golder (1995) was accurate within 18% and had a standard deviation of 35% with respect to the observed runout. The other three empirical tools produced less accurate predictions and are discussed in Section 4. The graphical prediction tools provided a simple and effective means of predicting runout, although inconsistencies arose with some of the case studies.

These results show that empirical and graphical runout prediction tools are best used with cases of similar conditions and settings to those which they were created from. They can reliably provide order of magnitude estimations of runout, but further development and testing is necessary before they can be relied upon for accurate estimates.

TABLE OF CONTENTS

1. INTRODUCTION 1

2. LITERATURE REVIEW 3

  2.1 Terminology 3

  2.2 The coal mine waste database 4

  2.3 Construction of mine waste dumps 5

  2.4 Mine waste dump stability 7

  2.5 Failure modes and mechanisms of mine waste dumps 8

  2.6 Flows and slides 10

  2.7 Parameters controlling runout 11

  2. 8 Empirical runout prediction methods 12

  2.9 Analytical runout prediction methods 16

  2.10 Failure prevention and mitigation 16

3. CASE STUDIES 19

  3.1 Aberfan, Whales - 1944, 1963, 1966 19

  3.2 Cilfynydd, Whales - 1939 21

  3.3 Jupille, Belgium - 1961 22

  3.4 Gold Quarry, Nevada - 2005 23

  3.5 South Field, Greece - 2005 25

  3.6 Anatolia, Turkey - 2001 26

  3.7 Summary of important case study parameters 28

4. RESULTS AND DISCUSSION 29

  4.1 Empirical predictions of travel distance 29

    4.1.1 Prediction of L_e as a function of volume 29

    4.1.2 Prediction of L_{toe} as a function of volume 31

4.1.3 Prediction of L_{toe} as a function of height 33

4.1.4 Prediction of Le as a function of volume 34

4.1.5 Prediction of H/L as a function of volume 35

4.2 Graphical predictions of H/L as a function of volume 37

4.2.2 Partly confined data 40

4.2.3 Confined data 42

4.2.4 All data 44

4.2.5 All confinement levels 46

4.3 Runout exceedence probability 47

4.3.1 Unconfined data 49

4.3.2 Partly confined data 51

4.3.3 Confined data 51

5. CONCLUSIONS AND RECOMMENDATIONS 53

ACKNOWLEDGEMENTS 55

REFERENCES 56

APPENDIX A 59

i.Aberfan 59

ii. Cilfynydd 61

iii. Jupille 62

iv. Gold Quarry 64

v. Greece 65

vi. Turkey 65

APPENDIX B 67

LIST OF FIGURES

Figure 1: Schematic definition of the fahrböschung …………………………………………..………... 4

Figure 2: Configuration of mine waste dumps depending on topography …………………...…………. 6

Figure 3: Conceptual model of the particle-size distribution seen in a mine waste dump constructed by the end dumping method ……………………………………………………………...…………… 7

Figure 4: Bar graph of typical dry densities for mine waste dumps 25

Figure 5.1: Regression results for the unconfined coal mine waste database ………………………...…38

Figure 5.2: Regression results for the unconfined data in the coal mine waste and new databases …..... 39

Figure 6.1: Regression results for the partly confined coal mine waste database ………………..…..... 40

Figure 6.2: Regression results for the partly confined data in the coal mine waste and new databases ...41

Figure 7.1: Regression results for the confined coal mine waste database ……………………...……42

Figure 7.2: Regression results for the partly confined data in the coal mine waste and new databases ...43

Figure 8.1: Regression results for coal mine waste database ……………………………………………44

Figure 8.2: Regression results for coal mine waste database and new cases ……………………..…..45

Figure 9: All confinement levels ………………………………………………………………...…46

Figure 10.1: Golder data (1995) – unconfined ……………………………………………...……...47

Figure 10.2: Golder data (1995) and new data – unconfined …………………………..……………..48

Figure 11.1: Golder data (1995) – partly confined ……………………………………..…………. 49

Figure 11.2: Golder data (1995) and new data-partly confined ………………………………………50

Figure 12.1: Golder data (1995) – confined ………………………………………….……………51

Figure 12.2: Golder data (1995) and new data – confined ……………………………………………52

LIST OF TABLES

Table 1: Coefficients for Formula 7 depending on volume and lateral confinement …………………... 15

Table 2: Case study parameters used for calculations ………………………………………………….. 28

Table 3: Additional case study parameters used for calculations ……………………………………… 28

Table 4: Input values for empirical formulas …………………………………………………………… 29

Table 5: L_e as a function of volume ……………………………………………………………...…30

Table 6: L_{toe} as a function of volume ……………………………………………………………..... 32

Table 7: L_{toe} as a function of height …………………………………………………………………. 33

Table 8: L_e as a function of V …………………………………………………………………….….. 34

Table 9.1: Equation for the prediction of H/L depending on confinement ……………………………... 36

Table 9.2: Equation for the prediction of H/L depending on confinement ………………………….….. 36

1. INTRODUCTION

Mine waste dumps, also known as overburden piles, stockpiles, spoil heaps and tips, are some of the largest man-made structures in the world. The instability of these structures can have an adverse affect on resource recovery, mining costs, safety, the natural environment and urban structures.

The most notable failure of a mine waste dump occurred in 1966 in the Welsh town of Aberfan, where a 67meter high tip failed and flowed into the town, killing 116 children and 28 adults. This catastrophic event served as a turning point in the mining industry. It forced the mining companies to pay closer attention to dumping practices and to treat the dumps as engineered structures which require close attention to design and ongoing monitoring. Fortunately, legislation following this tragic incident has amended tipping practice, but there is still much room for improvement.

Since 1966, there have been many waste dump failures all over the world. However, many of them were never reported since there is no mandatory requirement and it is not in the companies' best interest to do so voluntarily. As a result, the opportunity to learn from the failures is mostly limited to the ones that have acquired media attention.

From 1990 to 1995, The BC Mine Waste Rock Pile Research Committee created a database of 44 major coal dump failures in the Canadian Rocky Mountains that occurred in the previous 25 years. Their failure mechanisms and modes were analyzed and classified; the cases were modeled, and empirical models were created in order to provide more tools to estimate the risk of mine waste failures.

One method of assessing the potential hazard of a mine waste dump is to estimate the runout distance based on the failure mechanics of the initial slide. Several empirical, analytical and graphical methods have been developed in order to predict the magnitude of this runout. Some of the models have predicted runouts to an acceptable range, while many others proved to be undependable. A newer school of thought is focusing on a risk-based approach to prediction that presents the runout distances in terms of probability densities.

This report aims to test several previously-developed runout prediction tools on a new database consisting of eight mine waste failures which experienced catastrophic failures and developed into “rapid to extremely rapid” slides. A description and discussion of each case is provided in Section 3. The eight cases lie outside of the coal mine failure database, which is discussed in Section 2. Their post failure travel distances are predicted using several tools and the predictions are then compared to their measured values.

2. LITERATURE REVIEW

In 1990, representatives of industry; CANMET; the British Columbia Ministries of Environment, Lands and Parks; and Energy, Mines and Petroleum Resources formed the Mine Waste Rock Pile Committee to promote research and spread knowledge about mine waste dumps. From 1990 until 1995, nine papers on mine waste dumps were published regarding the design, monitoring, instability mechanisms and consequences of failure. These nine publications have set precedents in the field of mine waste disposal, and alongside the contributions of a few other individuals, are the foundation for this literature review. This literature review is a compilation of their arguments and ideas as well as those of others in the field, as they relate to the failure, and specifically, the runout of mine waste dumps.

2.1 Terminology

The variables and terms listed below are used throughout the report and are important inputs in the various formulas described in this paper.

As stated earlier, solid mine waste dumps have many synonyms. Specifically, in coal mining, they are referred to as spoils, spoil tips, spoil heaps or tips. The term “waste dump” has originated in North America and is commonly used in metal mining operations (MEMPR, 1992). Many people in the industry avoid the use of the term “waste” because there are undesired social connotations with the word, so the terms “overburden piles” or “mined rock piles” are generally preferred when communicating with the public. For the purposes of this report, the piles/dumps/tips will be referred to as mine waste dumps.

Runout, post-failure travel distance = the distance the deposit travels beyond the source

Fahrböschung, angle of reach, travel distance angle, runout angle, α = the angle below the horizontal from the crest of the failure to the toe of the deposit (Figure 1)

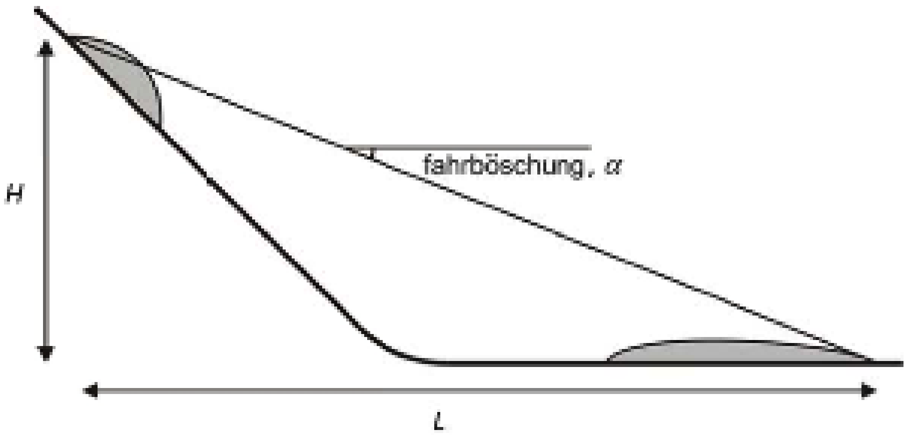

Figure 1: Schematic definition of the fahrböschung

V = volume of the deposit

H = elevation difference between the crest of the source and the toe of the deposit

B = width of the slide

R, RR = spreading ratios

$\mathbf{L_e}$ = excess travel distance; the horizontal displacement of the toe of the deposit beyond the distance one expects from a frictional slide down an incline with a normal coefficient of friction of tan (32˚), (Hsu, 1975)

$\mathbf{L_{toe}}$ = distance from the toe of the source slope to the toe of the deposit

**Note: L_e and L_{toe} are both measurements of runout distance

2.2 The coal mine waste database

The Canadian Rocky Mountain coal mines have been home to many waste dump failures due to their steep slopes and poor strength characteristics. In 1995, The British Columbia Mine Waste Rock Pile

Committee employed Golder Associates to create a database of failures. Forty four coal mine failures from 1970 to 1995 were reported and documented in detail. Several references to the 1995 Golder database will be made throughout this report.

Where the data was sufficient, each failure was analyzed, categorized and modeled in order to gain knowledge on the mechanics of these massive man-made structures. Comparisons were made with natural rockfall events and it was found that “preliminary comparison of data for the waste dumps and for major natural rock avalanches indicates broad similarities in their characteristics” (Golder, 1995). Allowing for a modification of characteristics and conditions, this finding enabled current knowledge about landslides to be applied to waste dump failures.

Golder’s study of the coal mine database lead to the development of several empirical runout prediction tools and has greatly furthered the understanding of mine waste failures. However, there is still much to learn, as their runout prediction methods have not been tested outside the confinement of the Canadian Rocky Mountain cases.

2.3 Construction of mine waste dumps

The shape of a mine waste dump is almost always determined by the topography of the placement zone. There are five main configurations and a variety of combinations of these (Zahl et al., 1992). They are shown in Figure 2 below.

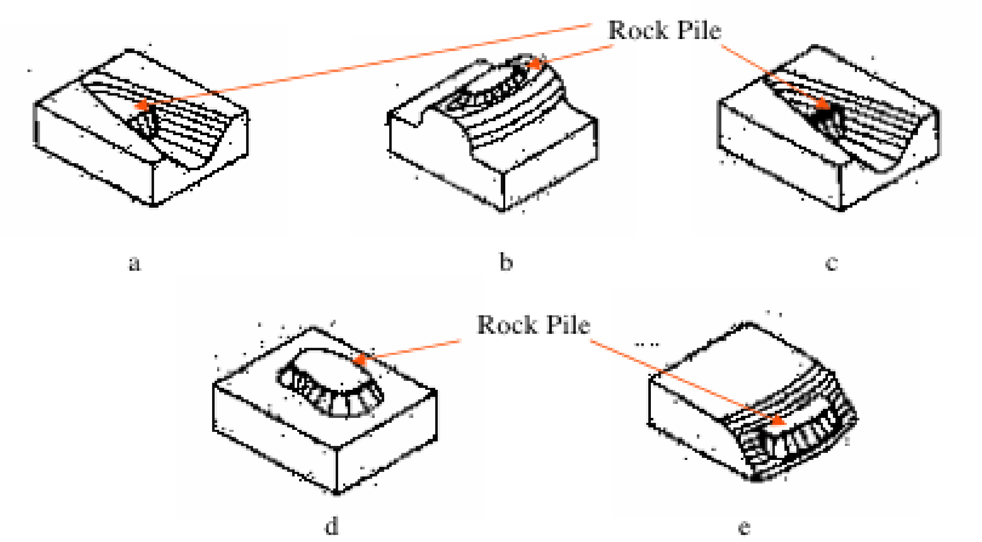

Figure 2: Configuration of mine waste dumps depending on topography (Zahl et al., 1992).

(a) Valley-fill **(b)** Ridge **(c)** Cross-valley **(d)** Heaped **(e)** Side-hill

The waste dumps themselves are classified by their construction method, depending on whether it is ascending or descending construction.

Ascending construction requires the development of lifts starting from the base, moving upwards, whereas **descending construction** refers to the placement of material from operating height and allowing the dump to develop naturally at its angle of repose (MEMPR, 1992). For coal mines, the angle of repose for descending structures has typically been 38˚ (Golder, 1995).

Free dumping is an example of ascending construction. The waste is dumped in small piles, graded, compacted and placed in lifts, resulting in denser layers than the descending methods. The other ascending methods are drag-line spoiling and mixing of the waste rock with tailings.

End dumping and **push dumping** are two types of descending construction, and they are often the cheapest. In end dumping, the mine waste is simply dumped from the truck at the edge of the dump site and the material is allowed to deposit itself along the slope face. Push dumping is similar but involves levelling of the dumped material by a tractor.

Nichols (1987) was the first to notice that all these methods can result in particle size segregation as the coarse grains move to the bottom of the dump and the fine grains remain at the top, as shown in Figure 3 below. A benefit of this segregation is the simultaneous construction of a drain at the base, which increases the permeability and the stability of the dump. More information on this stratification mechanism can be found in McLemore et al. (2005).

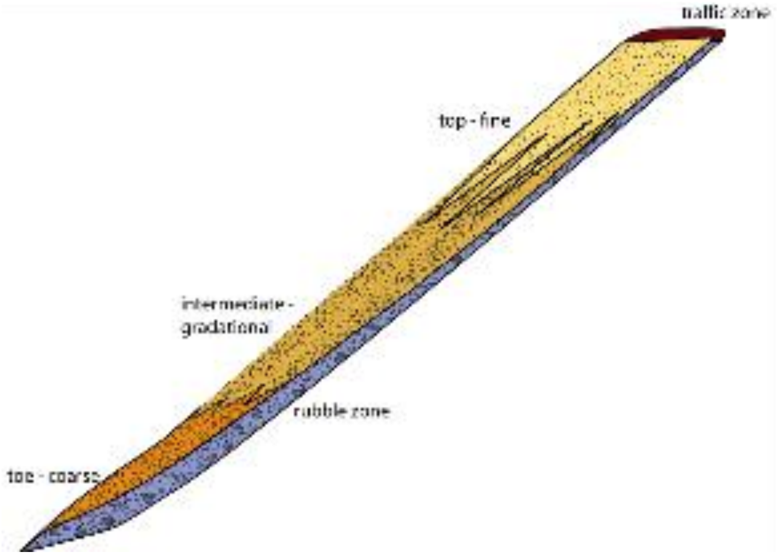

Figure 3: Conceptual model of the particle-size distribution seen in a mine waste dump constructed by the end dumping method (Nichols, 1987)

2.4 Mine waste dump stability

The stability of a mine waste dump depends on factors similar to other embankments: snow/ice conditions, foundation conditions, material quality, loading rate, topography and piezometric conditions. Therefore, there are numerous ways for instabilities to occur.

To calculate the stability of a waste dump, the failure mode must be anticipated. This can be difficult since the mode can be outside the realm of the simplified parameters assessed in the design (MEMPR, 1992). Often, a generalized slip surface is assumed and the lowest safety factor is estimated using limit equilibrium methods of stability assessment. Another governing factor is that most waste dumpsare heterogeneous and anisotropic. This fact proves to be problematic sincethe limit equilibrium methods often yield erroneous results due to their inability to link stress and strain events (MEMPR, 1992).

It is interesting to note that the 1995 Golder database contained only coal waste failures, which consist of sedimentary rocks that are often weaker and weather differently than metamorphic and igneous deposits. Overall, sedimentary waste dumps will act differently than igneous or metamorphic deposit dumps, which enforces the need to test the runout prediction methods on non-sedimentary waste dumps.

2.5 Failure modes and mechanisms of mine waste dumps

The failure modes of mine waste dumps are controlled by the behavior of the natural strata on which they are founded and by the properties of the tipped material (Bishop, 1973). Seven failure modes were identified in Review and Evaluation of Failures by MEMPR (1992).

Below is a brief summary of the failure mode and mechanism frequencies of the coal mine database, as they were categorized and calculated by MEMPR (1992).

Yielding toe/Toe failure (YT) is described as local instability in the toe of the dump, which can be due to weak foundation soils at the toe, steep foundation slopes in the toe area or high foundation pore pressure. These failures are the most common and often lead to subsequent failures of greater magnitudes, possibly of the entire dump. The failure mechanism for this mode is the massive redistribution of the load within the moving material (MEMPR, 1992).

Basal failure (B) is characterized as a failure along a plane of weakness at or near the foundation contact zone. This includes pseudo-rotational, planar or block translation displacement that occurs at the foundation contact at a relatively shallow depth (MEMPR, 1992).

Rotational embankment failure (Re) is characterized by deep rotational failure of the mine waste itself, excluding the foundation. It occurs due to the weak homogeneous nature of the waste material, infiltration or foundation seepage elevating the pore pressure (MEMPR, 1992).

Rotational foundation failure (Rf) is the mass failure of the dump material and the foundation material together. The common cause is high foundation pore pressures (often due to rapid loading) and weak foundation soils (MEMPR, 1992).

Sliver failure (S) is failure is due to poor material quality (often fine-grained) and rapid loading rates. The abundance of fines can cause apparent cohesion that can result in over steepening of slopes (43° has been recorded) (MEMPR, 1992). This failure mode is common and displaces relatively low volumes.

Liquefaction/Translation (L/T) often occurs in low-lying topography with shallow foundation slopes. Common site characteristics are fine-grained zones where pore water is not readily dissipated. Rapid loading and seismic activity can cause liquefaction of the silt or sand layers, although seismic activity has not been reported as a failure mechanism for this mode. This failure mode is discussed in greater detail in the next sub-section.

Planar failure (P) occurs on a discreet plane of weakness within the dump material. This can occur wherever the internal strength of the dump is exceeded (MEMPR, 1992).

MEMPR (1992) grouped the failures into primary and secondary modes of failure where a second mode was evident. They found that yielding toe failures (YT) were the most abundant primary failures in both frequency (29.5%) and in terms of volume percentage (66.8%). Basal failures (B) were the second most common primary failure modes (20.5%, 13.7%). For secondary modes of failure, planar failures (P) were the most frequent (42.3%) but basal failures (B) were responsible for the most failed volume (59.7%).

The most frequent failure mechanisms were: poor quality material (18%), high loading rate (14%), steep topography (9%), followed by high pre-failure precipitation, unconfined toe and excessive pore pressure generation.

Other important facts to note about the failures in the database are that almost all of the slides occurred on active dumps during the placement of waste (Golder, 1995). Secondly, each failure in the coal mine database was preceded by substantial horizontal and vertical deformation of the dump crest, which could have been, or can now be, anticipated through the use of wireline extensometers (MEMPR, 1992).

2.6 Flows and slides

Many of the landslides with the longest displacements recorded assume a flow-like character (Golder, 1995). If the landslide consists of sensitive clays, is acting at or above the liquid limit and liquefies to an extremely rapid pace, then it is classified as a **clay flow slide** (Hungr et al., 2001). Similarly, if the landslide contains sand, debris, silt or weak rock; is saturated at the rupture surface and liquefies to an extremely rapid pace; it is known as a **sand (silt, debris, rock) flow slide** (Hungr et al., 2001). **Debris flow** is a landslide consisting of saturated debris that travels in an established channel at an extremely rapid pace (Hungr et al,, 2001). A characteristic of a debris flow is that the slide loses its original structure, which is opposite a **debris slide**, which keeps its original structure throughout the slide.

The high mobility of debris flows and flow slides is often explained by liquefaction of the fully saturated, loose, fine-grained debris (Golder, 1995). In the high mobility case, “slide lubrication by liquefied material appears to be a dominant mechanism which controls slide runout in most mobile [waste dump failure] events” (Golder, 1995). As for the failure mechanisms, there are a number of hypothetical mechanisms that attempt to explain the high mobility. The two leading mechanisms are undrained loading pore pressure effects and acoustic fluidization (Golder, 1995). Acoustic fluidization is analogous to the shearing of sand on a vibrating surface, which acts to decrease friction (Melosh, 1979).The susceptibility of a dump to static liquefaction is largely dependent on the structure, relative density, degree of saturation and permeability of the soil and the effective stress conditions imposed (Hunter and Fell, 2003). The flow behavior of the debris flows and flow slides is primarily controlled by the boundary conditions and the flow path, and less so by the slide material properties (Golder, 1995). However, contractive soils, which are normally consolidated, are at a much higher risk of liquefying than dilative soils, which are overconsolidated (Hunter and Fell, 2003).All the cases presented in this report are either flow slides or debris flows. Debris slides are uncommon because most slides that are initiated in dilative soils lose their original structure and take on the flow-character described above. For a debris flow to occur in dilative soils, a slope steeper than 25° must often be present. In soils that are contractive on shearing, landslides will always reach a 'rapid' post-failure velocity (Hunter and Fell, 2003) and are usually flows.

2.7 Parameters controlling runout

Golder (1995) identified several parameters that control the runout of a mine waste dump failure: the longitudinal path profile, the transverse path geometry, the runout path mantle, the dump dimensions, and the waste material. Each one of these parameters is briefly discussed below.

The **longitudinal path profile** describes the length and steepness of the runout path. A long, steep path is conducive to a long runout and a short, flat path that runs into an adverse slope will not have a very long runout.

The **transverse path geometry** describes the level of lateral confinement (i.e. confined, partly confined and unconfined). The length of runout usually increases with a higher degree of confinement. A definition of each confinement level is presented below as per Golder (1995).

Confined -	the runout path is constrained by the relatively steep side slopes of a gully or small valley, and has constant or reducing width along most of the path.

Partly Confined -	the runout path is not sharply defined by a topographic depression, and has a constant or gradually increasing width with decreasing elevation.
Unconfined -	the topography of the runout path permits or encourages widening of the slide debris from an early stage.

The **runout path mantle** describes the characteristics of the material at the base of the slide. Most waste dump slides pass over bedrock, colluvium, glacial till or older waste. These materials each have an effect on the runout distance, but none are as influential as a path mantled by a natural depression or drainage channel. These channels usually contain highly saturated loose alluvial or organic material and are extremely conducive to very mobile sliding events (Golder, 1995).

The **dump dimensions** include the elevation loss of the slide and the volume of the mobilized material. Both of these parameters are highly correlated to the runout distance and are the basis of most empirical formulas.

The last parameter affecting the runout is the **waste material**. This parameter does not appear to have a large influence on mobility once the slide begins; however, it is a very important factor in the initiation of failure (Dawson et al, 1998).

2. 8 Empirical runout prediction methods

The factors affecting landslide mobility and travel distance are very complex and difficult to account for; therefore, empirical models and graphical correlations are very useful methods in predicting runout distances. The correlations for landslides form the basis for mine waste failure mobility and runout/travel distances.

Heim (1932) was the first to notice that volume was directly proportional to landslide mobility [although some now believe that the mobility is not dependent strongly on slide volume (Golder, 1995)]. Future research by Scheidegger (1973), Abele (1974) and Hsu (1975) would eventually lead to the creation of the term excess travel distance, L_e, which is supposed to estimate the total length of the deposit

$$L_e = L-H/\tan(32) \qquad (1)$$

Combined with a spreading ratio factor, R, an equation was developed to provide a family of curves for more and less mobile rock avalanches. Hungr (1990) later found good correlation between log (H/L) and log (V).

Golder (1995) later proposed a method of empirical runout prediction for waste failures that considered lateral confinement, volume of the mobilized material and two spreading ratios, R and RR. The results of their analysis concluded that all of the waste failures could essentially be grouped into two classes: normal and more mobile events

A summary of the three empirical runout prediction formulas developed by Golder (1995) are shown below.

Excess travel distance, L_e, with slide volume, V

$$Le = (74.5 * R)^{1/2} * (V)^{3/4}, \text{ Normal event} \qquad (2.1)$$

$$Le = (22.8 * R)^{1/2} * (V)^{1/3}, \text{ Highly mobile event} \qquad (2.2)$$

$$\text{Where } R=L_e/B \qquad (2.3)$$

Travel distance beyond dump toe, L_{toe}, with volume, V

$$L_{toe} = (RR * c * V^n)^{1/2} \qquad (3.1)$$

Where $RR = L_{toe}/B$ (3.2)

Travel distance beyond dump toe, L_{toe}, with height, h

$$L_{toe} = [(c * R)^{½} * (e^{((h+G)/D)})^{1/N} + E]/F \qquad (4)$$

One of the key problems with formulas (2.1), (2.2), (3.1) and (4) is that they do not take into account the slope angle that the dump rests on.

Li (1983) correlated rock avalanche deposit area with volume for over 70 cases in Europe. The resulting empirical equation was

$$\text{Log } A = 1.9 + 0.57 * \log V \qquad (5)$$

Equation 5 was then combined with Hungr's (1990) assumption of a bilinear runout profile and the spreading ratio, R, to come up with the following equation (Golder, 1995):

$$L_e = R^{0.5} * 10^{0.95} * V^{0.28} \qquad (6)$$

Corominas (1996) presented another prediction method when he analyzed data for 204 landslides in soil and rock. He found correlation between the ratio of elevation difference to travel length, H/L, and slide volume, V, as was postulated earlier by Hungr (1990) and a few others. Most of the correlations were seen for slides with large volumes, with magnitude of 10^7 and larger; while the smaller volume slides showed significant scatter. The equation is shown below, alongside a table displaying the values of the coefficients for the equation (Corominas, 1996).

$$H/L = AV^B \qquad (7)$$

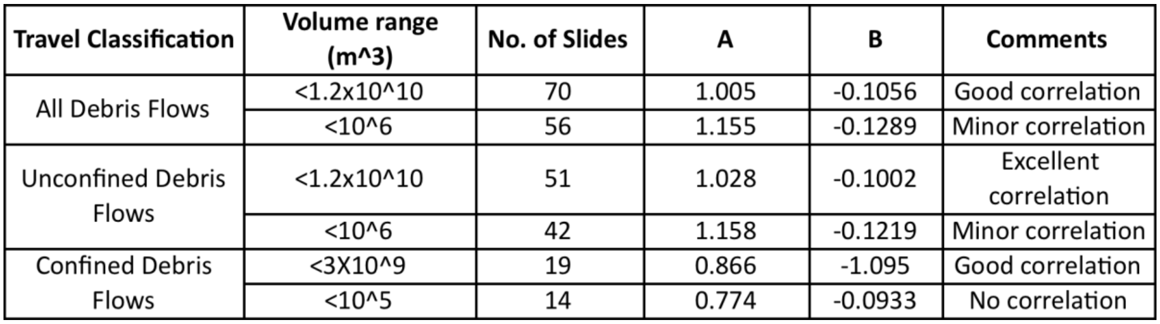

Travel Classification	Volume range (m^3)	No. of Slides	A	B	Comments
All Debris Flows	<1.2x10^10	70	1.005	-0.1056	Good correlation
	<10^6	56	1.155	-0.1289	Minor correlation
Unconfined Debris Flows	<1.2x10^10	51	1.028	-0.1002	Excellent correlation
	<10^6	42	1.158	-0.1219	Minor correlation
Confined Debris Flows	<3X10^9	19	0.866	-1.095	Good correlation
	<10^5	14	0.774	-0.0933	No correlation

Table 1: Coefficients for Formula 7 depending on volume and lateral confinement

Although the aforementioned formulas provide order magnitude predictions of runout distance, it is believed that they need to be moderated by engineering judgement and should not be the sole factor for decision-making when applied to a mine waste dump with different characteristics and setting to the ones that were used to design the formula.

Like many models, the formulas listed above are oversimplifications of a complex system. One of the limitations inherent to the models is that they do not take into account the slope angle of the path mantle. Hunter and Fell (2003) use α_1, α_2 and α_3 along the slope mantle to properly describe the angles. This addition greatly increases the accuracy of the prediction. Another difficulty with the empirical models is that they require the input of parameters that are often unavailable, or difficult to assess.

The accuracy of Formulas 2.1, 2.2, 3.1, 4, 6 and 7 will subsequently be tested on the eight cases presented in this report.

A representation of Hungr's postulated correlation of log (V) versus log (H/L), alongside a runout exceedence probability estimate will also be applied to the Golder database and to the eight new cases. The graphs will serve to show the regression and probability results before and after the addition of the new data. These tools can be very useful in runout prediction since they are simple, transparent, can provide a risk assessment deliverable to a client and acknowledge the broad range of possible outcomes.

2.9 Analytical runout prediction methods

Similar to the abundance of empirical prediction models, there are several analytical models that can be used to assess the risk of mine waste dump failures. One such model is DAN, a numerical model created by Hungr (1995). DAN is a numerical continuum model used for the dynamic analysis of flowing materials. It is based on consideration of the energy balance in the post-failure stage, as is described by Lerouil (1997), and it “uses a moving reference frame to simulate the deformations and translation of cells of fixed mass which comprise the slide” (Golder, 1995). The outputted runout predictions of this model are very sensitive to the rheological model and to the parameters used in the numerical model.

Golder (1995) used DAN in addition to the empirical models to accurately predict the travel distances of many of the mine waste dump failures in their database. It proved that DAN is very useful when calibrated against historical events with similar soil types, morphological, topographical and climatic conditions (Hunter and Fell, 2003).

Analytical models serve as very useful tools in runout prediction and their use is suggested in combination with empirical methods. Both analytical and empirical methods should be applied with judgment and explicit uncertainty bounds.

2.10 Failure prevention and mitigation

When proper attention and care is given to the construction and monitoring of a mine waste dump, failures can be prevented. In their 1995 report, Golder mentioned that all the mine waste failures occurred on active dumps during placement. They also stated that all the failures were preceded by substantial horizontal and vertical deformation of the dump crest. One of the ways that failures can be anticipated is by means of wireline extensometers, which are relatively easy to use and cost-effective.

There are also several mitigation methods that can be used to reduce the risk of mine waste failure. They are: proper drainage, stabilization of the toe, compaction of the material, slope flattening, sound foundation prepping practice, wireline extensometers as monitoring-practice, berms and barriers, and warning systems.

3. CASE STUDIES

Eight case studies are presented in this section. They consist of mine waste failures that occurred in Whales, Turkey, USA, Greece and Belgium within the last century. The BC Mine Waste Rock Pile Research Committee has not analyzed any of the cases presented in this report in the nine publications written from 1990-1995, so they are perfect test subjects for the empirical models.

Six of the mine waste dumps were derived from coal mining operations while the other two were gold and fly ash. The setting in which the failures occurred is also very different from that of the BC Rocky Mountains. Thus, it is of interest to see if the cases presented in this report apply to the models created by Golder (1995) and Hunter & Fell (2003). The failure modes, mechanisms and a brief history of each case is presented below, where the information was available. The key parameters are mentioned and a table summarizing them is shown at the end of the section.

3.1 Aberfan, Whales - 1944, 1963, 1966

The Merthyr Vale Colliery spoil heap is located in the Welsh town of Aberfan, which is home to three historical failures of solid mine waste, which are described in this section. The failures occurred in 1944, 1963 and 1966. All three were flow slides, although the 1944 and 1966 flow slides eventually turned into debris flows.

The 1944 failure occurred on Tip 4 whilst the later two occurred on Tip 7. In all cases, a rotational slide occurred on an active tip and turned into a flow slide.

The 1944 flow slide contained 230,000 – 265,000 cubic meters of material and the 1963 flow slide contained 23,000 cubic meters. Their elevation losses were 194 and 120 meters respectively while their runout widths were approximately 85 and 60 meters respectively.

The 1966 failure of the Aberfan tip is well known in the mining industry as the disaster that changed solid mine waste practice forever. The Welsh town of Aberfan hosted a coal mine that practiced tipping as a means of solid waste disposal. When the dump failed in 1966, 108,000m^3 flowed, from the reactivation of an old slip-surface, into the town killing 116 children and 28 adults. Most of the children were in the age range of 7-10.

In 1963, tailings were introduced to Tip 7. Its peak angle of friction was 32 degrees and it had a permeability of 1.73x10^{-7} cm/s. This addition of tailings to the dump proved to be very problematic and was definitely a contributing factor to the failure, as it created perched water tables and thus increased pore pressure and decreased the effective stresses.

The foundation material was boulder clay with an internal friction angle of 36 degrees. The waste material was primarily shale, which is friable and easily disintegrates, and had a friction angle of 39 degrees with a residual friction angle of 18 degrees, which was seen at the failure surface. The permeability of the waste dump was 6.6x10^{-2} cm/s.

Among the aforementioned issues, there were many other problems with the dumping practices at Aberfan. For one, the tip was under-compacted, having 82% SPM while needing a 95% SPM. Therefore, when a large shear force was applied, the volume of the tip greatly decreased. This large decrease in volume was the cause for the increase in pore pressure. This fact, in addition to the high brittleness of the waste material, was the cause of the vast movement of the sliding material (Bishop, 1973). Secondly, the tip was constructed at an angle similar to its internal friction angle. Thirdly, no drainage measures were employed which caused a reduction in the effective stress at the toe. Furthermore, deformations in the dump were seen at 50 meters but the dump was built until a height of 67 meters. These deformations support the hypothesis that these failures typically show indications of instability prior to failure.

Lastly, right before the failure occurred, fissures had caused high artesian pressures. A pore pressure of 20 feet was measured after the failure and only 23 feet was needed to induce failure. So, this high pore pressure was one of the more influential factors causing the failure.

The failure flowed 600 meters down an elevation loss of approximately 180 meters in a partly confined channel into the town at an approximate velocity of 8-11m/s (Hutchinson, 1986) which is considered to be extremely rapid (Hungr, 2001).

More information on the Aberfan cases can be found in Bishop (1973) and Siddle et al. (1996).

3.2 Cilfynydd, Whales - 1939

The Ropeway tip at Cilfynydd Common was located a few miles South of Aberfan in Whales. In 1939, the tip underwent a rotational slip that was most likely triggered by a rise in pore pressure at the base of the flow slide (Siddle et al, 1996). The slide consisted of 180 000 tons of colliery waste and would have been as destructive as the 1966 Aberfan failure had there been similar infrastructure in the runout path (Siddle et al, 1996). The normally consolidated, contractive soil turned into a flow slide and covered the Cardiff-Merthyr road for five days, blocking and diverting the canal and the River Taft. It also cut a railway and compressed air main.

The runout spanned approximately 460 meters from the toe and 600 meters from the crest. The tip measured approximately 45 meters high and the elevation loss of the failure was 134 meters at about 36 degrees down slope.

The slide was observed by a motorist; whose remarks allowed Bishop et al (1969) to approximate the velocity of the slide to an order of magnitude of 10 mph, or 4.5 meters per second, which is classified as extremely rapid by Hungr (2001). Movement of the slide eventually slowed and occurred for ten minutes.

The steepness of the runout path mantle was similar to that of the BC Rocky Mountain cases and the lateral confinement was classified as being confined, which generally yields the longest runout distances. Lastly, the slide was observed as not being particularly wet.

More information can be found in Bishop (1973) and Siddle et al. (1996).

3.3 Jupille, Belgium - 1961

The Fly Ash waste dump in Jupille, Belgium was created by the ascending construction method as it was tipped by truck without compaction. Between 100,000 and 150,000 cubic meters of material was mobilized in the flow slide that occurred in the normally consolidated, contractive soil (Bishop, 1973). For calculation purposes, a median volume of 125,000 cubic meters has been assigned to the slide.

The elevation loss of the slide was the highest reported of the eight cases presented in this report: 1470 feet. The runout of the slide was laterally confined by berms and trenches and enabled the slide to travel into the town of Jupille, where it killed eleven people and destroyed many houses.

The slide occurred on February 3, 1961 and travelled down an 18 degree slope for approximately 2000 feet and reached speeds as high as 100 mph. The failure mode is believed to be a translation but not liquefaction since statements given at the time of the failure suggested an airborne flow slide as opposed to a liquefaction slide. This is odd considering the water content of the tip may have reached as high as 58% when the lower part of the tip was saturated by flowing surface water that travelled over an impervious clay layer. When the steep, slightly cohesive tip was undermined, the tip collapsed and there was a breakdown in the honeycomb structure of the fly ash. This enabled the slide to be effectively in suspension.

The mobility of the Jupille case was extraordinary considering the volume of activated material. A possible explanation for this is the properties of fly ash and its ability to be easily suspended in air.

More information can be found in Bishop (1973).

3.4 Gold Quarry, Nevada - 2005

Newmont Mining Corporation is the owner of the Carlin Surface mine operation in Northern Nevada. Large-scale mining began in the Gold Quarry Open Pit in the early 1980's. On February 5th, 2005, approximately 9.1 Megatonnes of material from the North Waste Rock Facility (NWRF) failed (Sheets and Baits, 2008). The slide buried 460 meters of Nevada State Route 766 when displacement of the toe of the slide reached 183 meters with no lateral confinement. The runout distance from the crest of the dump was 655 meters.

Initial mining of the Gold Quarry Open Pit uncovered three distinct rock sequences, all of which consisted primarily of sedimentary rocks or volcanoclastics. The middle layer of the Carlin Formation was the major source of the waste rock. During placement of the waste, the Carlin Formation was placed at the base of the NWRF and is the primary unit of interest in understanding the cause of the failure (Harlan et al. 1999; Regnier 1960).

The slope of the NWRF was at its final design configuration of nearly 3H:1V, with a crest to toe elevation difference of 128 meters. The mine waste dump was constructed in three lifts of approximately 24 meters of highly plastic, tuffaceous material. A sulfide stockpile, which was eventually converted to waste, overlaid these three lifts and was approximately 55 meters high. The construction method was descending and end dumping was used to create the mine waste dump.

Following the failure in 2005, a geotechnical investigation was conducted to determine the factors that resulted in the catastrophic failure of the waste dump. It included eight boreholes and six test pits for bulk samples and vibrating wire piezometers to model the pore water pressures. The water table was found to be at approximately 10 meters below the surface topography (Sheets and Baits, 2008). The failure surface was found to be in the lowest portion of Lift 1 near the native ground contact.

The lower lifts were composed of montmorillonite-rich clays. These are characterized as being weak, high- plasticity, clay-silts. The high percentage of fines content in the waste material made the waste dump highly prone to slope instabilities (Sheets and Baits, 2008). It is believed that this weak layer was the predominant factor that resulted in the NWRF slope failure (Sheets and Baits, 2008).

Furthermore, Atterberg limits indicated that the majority of the samples from lifts one to three were high plasticity silts, which can exhibit strain-softening behavior. This behavior is characterized by a continuously reduced strength with continual deformation until the strength is brought to a residual value.

Preliminary stability analyses of the post-slide conditions were conducted to determine the variations in residual strength of the dump. Cross sections of the pre-failure geometry determined that the residual factors were 61% and 68% for two possible conditions analyzed. Both conditions displayed factors of safety in the failing range, with 0.79 for a pore pressure condition and 0.85 for a non-pore water pressure condition (Sheets and Baits, 2008).

Since only slide tonnage was reported in the failure reports, a density was required to determine the failure volume. Figure 4 (McLemore et al, 2005) below shows typical mine waste dump densities around the world. For this report, 2.0 g/cc was chosen as the dry density.

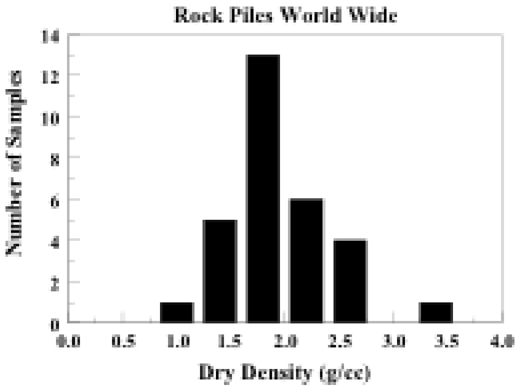

Figure 4: Bar graph of typical dry densities for mine waste dumps (McLemore et al, 2005)

3.5 South Field, Greece - 2005

South Field Mine is the largest open pit mine in Greece. The mine covers an area of $24km^2$ and operates on ten benches at a time using the continuous mining method. From 1979 to 2005, it produced 310Mt of lignite and excavated nearly $1200Mm^3$ of overburden and interbedded waste (Steiakakis et al, 2008).

The waste was a mixture of interbedded and soft overburden material. It was moved from the mine to an external waste dump by conveyor belts where it was deposited, often without preconsolidation, in three phases and reached a height of 110 meters at a 10% inclination (5.8degrees). The dump consisted of fine-grained (mostly clay) materials with a low friction angle and high water content.

On April 2005, $40Mm^3$ of the dump failed and flowed 1100 meters with a thickness between 30 and 90 meters. The width of the slide was approximately 550 meters.

A 20-meter high dam was created to stop the rapidly moving deposit but it was abandoned as the deposit moved quicker than had anticipated and overtook the dam. The deposit then moved another 300meters until it ran into a second dam, which stopped the sliding mass. Had the first dam not slowed down the deposit and the second one not stopped it, the runout distance could have been much longer. Contrarily, the longitudinal path was 2-3 degrees in favor of stability; so one would presume that the runout should not have been as long as it was, even without the mitigation efforts.

Post-failure drilling discovered an aquifer directly underneath the waste dump. At that location, the hydraulic head fluctuates 30 meters from summer to winter. The pressure in this aquifer transmitted into the dump and built up a pore pressure of 1000kpa by the end of winter, 2004 (Steiakakis et al, 2008). This pre-failure pore pressure exceeded the mean annual value.

Using the SEEP/W software, engineers discovered that the pore water pressure built up in the conglomerate formation and propagated into the waste dump deposit. However, despite this fact, a stability analysis completed before the failure showed that the long-term stability was still greater than the required 1.5 (Steiakakis et al, 2008).

This failure shows the importance of investigating the hydrogeologic conditions and the strength of the spoil material near the base; as it is a key factor for the stability and design of preventative measures (Steiakakis et al, 2008).

3.6 Anatolia, Turkey - 2001

One of Turkey's largest mines is a strip coal mine in Central Anatolia. The mine has been in production since 1988 and produces 3.8 million tons of lignite per year. In June 2001, a large failure occurred in the Central pit. The failure was classified as rapid and covered an area of 0.3 square kilometres (Ulusay et al., 2005).

The pile was end-dumped at its natural angle of repose of 35 degrees with an overall slope of about 12 degrees. The height of the spoil pile was 115 meters, consisting of several benches. There was no lateral confinement for this failure (Ulusay et al., 2005).

The geology of the mine consists of two 7 meter coal seams with 20 meters of interburden that is excavated by a 50m^3 walking dragline. The overburden is 80 meters and is excavated by smaller 15m^{3}electrically operated excavators. This layer consists of marls, karstic limestones and sandstones. The interburden consists mostly of damp, weak to very weak clayey silts.

X-ray diffraction analyses show that clays and silts dominate the overburden, interburden, foundation materials and in-situ slope forming material. The high fines content of these layers was one of the contributing factors of failure.

Meteorological records indicate that there was high intensity rainfall in May, one month before the failure occurred. Despite dewatering efforts, water could not be removed from the overburden due to low permeability of the materials. Furthermore, water flow and pools were observed at different benches and on the pit bottom. Drill holes later confirmed the presence of a water table 5 to 17 meters below the surface of the dumps. Therefore, the influencing factor to the failure is believed to be heavy rainfall prior to the failure and the failure mechanism is believed to be compound failure (Kasmer et al, 2005), as is illustrated in Appendix A.

The failure mode was primarily translation of the toe, followed by secondary circular failure through the dump and planar failure through the foundation. Post-failure material testing suggests that the shear strength of the dump and foundation-interface materials were at or approaching residual values and had no cohesion.

Similar to the other failures discussed in this report, signs and warnings of an imminent failure were present. In this case, large tension cracks were seen at the crest of the failure days before it occurred.

Approximations from plan view photos taken at the time of the failure provide a value for width: 200 meters. This value is important since it enables the calculation of the spreading ratio.

3.7 Summary of important case study parameters

Event	Volume V (m^3)	Width W (m)	Runout from Toe L_{toe} (m)	Runout from Crest L (m)	Crest to Toe Elev. Diff. H (m)	H/L	L/H
South Field, Greece	40.000.000	550		1100	110	0,100	10,00
Anatolia, Turkey	20.000.000	200		600	115	0,192	5,22
Gold Quarry, Nevada	4.155.000	460	183	655	128	0,195	5,12
Aberfan, 1966	108.000	150	550	600	180	0,300	3,33
Aberfan, 1944	245.000	85	358	588	194	0,330	3,03
Aberfan, 1963	23.000	60	230	345	120	0,348	2,88
Cilfynydd, Whales	104.000	130	460	600	134	0,223	4,48
Jupille, Belgium	125.000	30		500	460	0,920	1,09

Table 2: Case study parameters used for calculations

Event	Fahrboschung	$\log_{10}(V)$	$\log_{10}(H/L)$	Confinement
	α (°)			
South Field, Greece	5.71	7.60	-1.00	Unconfined
Anatolia, Turkey	10.85	7.30	-0.72	Unconfined
Gold Quarry, Nevada	11.06	6.62	-0.71	Unconfined
Aberfan, 1966	16.70	5.03	-0.52	Partly Confined
Aberfan, 1944	18.26	5.39	-0.48	Confined
Aberfan, 1963	19.18	4.36	-0.46	Confined
Cilfynydd, Whales	12.59	5.02	-0.65	Confined
Jupille, Belgium	42.61	5.10	-0.04	Confined

Table 3: Additional case study parameters used for calculations

4. RESULTS AND DISCUSSION

This section contains the predictions of the empirical formulas as well as the graphical tools, which are all applied to the eight new cases and in certain instances, to the 1995 Golder database.

4.1 Empirical predictions of travel distance

4.1.1 Prediction of L_e as a function of volume

The first formulas tested in this report are Formulas 2.1 and 2.2 (Golder, 1995):

$$Le = (74.5 * R)^{1/2} * (V)^{3/4}, \text{ Normal event} \qquad (2.1)$$

$$Le = (22.8 * R)^{1/2} * (V)^{1/3}, \text{ Highly mobile event} \qquad (2.2)$$

These formulas take volume and spreading ratio as inputs, and output a value of excess travel distance. The spreading ratio, R, is estimated based on the length and the width of the slide, which, for this report is equal to a calculated excess travel distance [L_e = L-H/tan(32)] divided by the width, b.

The input values are shown in Table 4 below.

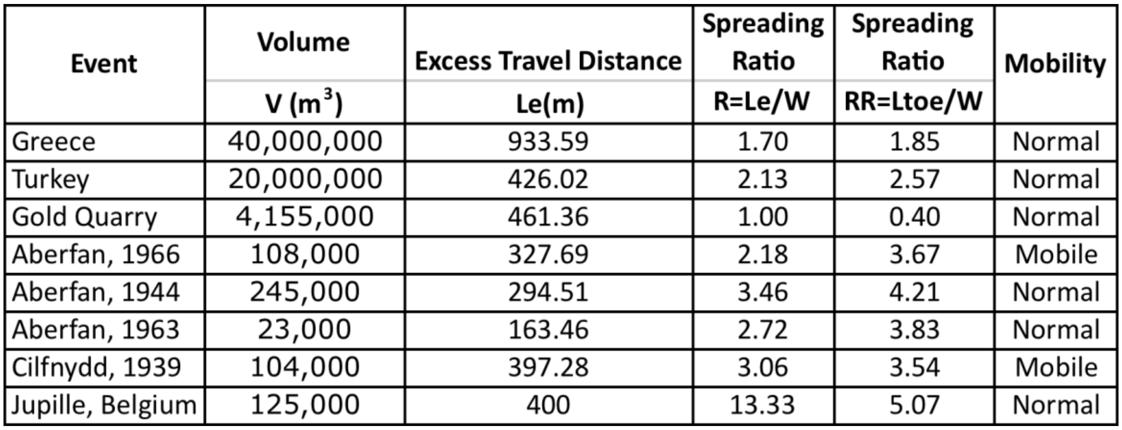

Event	Volume	Excess Travel Distance	Spreading Ratio	Spreading Ratio	Mobility
	V (m^3)	Le(m)	R=Le/W	RR=Ltoe/W	
Greece	40,000,000	933.59	1.70	1.85	Normal
Turkey	20,000,000	426.02	2.13	2.57	Normal
Gold Quarry	4,155,000	461.36	1.00	0.40	Normal
Aberfan, 1966	108,000	327.69	2.18	3.67	Mobile
Aberfan, 1944	245,000	294.51	3.46	4.21	Normal
Aberfan, 1963	23,000	163.46	2.72	3.83	Normal
Cilfnydd, 1939	104,000	397.28	3.06	3.54	Mobile
Jupille, Belgium	125,000	400	13.33	5.07	Normal

Table 4: Input values for empirical formulas

The Jupille case is a great example of the inherent problems with the use of excess travel distance, L_e, as an indicator of runout. Since the travel angle of the slide was so high, 43°, it leads to a calculated L_e of -196 meters. Clearly, in this case, excess travel distance does not correctly approximate the length of the deposit, as the travel distance must be a positive value. To make up for this fact, the excess travel distance was assumed to be 80% of the runout-from-crest measurement (500 meters). This assigned L_e value enables the upcoming runout predictions to be made.

Table 5 below shows the predictions for excess travel distance based on Formulas 2.1 and 2.2 and the % difference with respect to the measured excess travel distance. The mobility was chosen based on which prediction was closest to the calculated value.

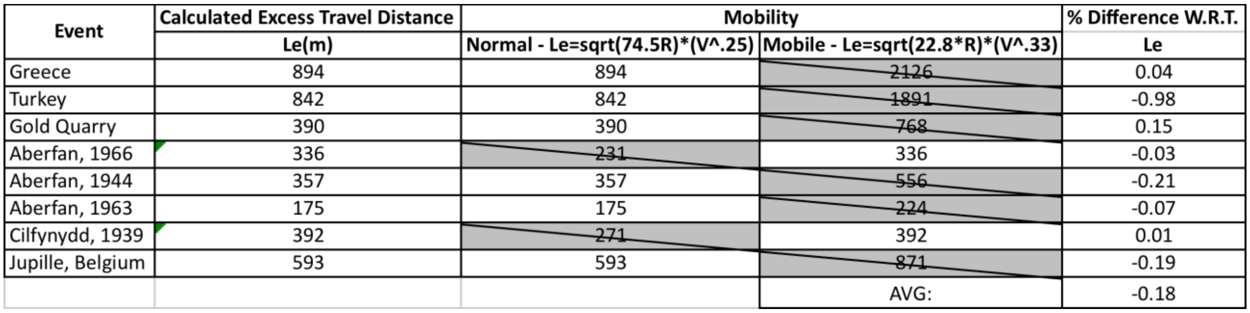

Event	Calculated Excess Travel Distance	Mobility		% Difference W.R.T.
	Le(m)	Normal - Le=sqrt(74.5R)*(V^.25)	Mobile - Le=sqrt(22.8*R)*(V^.33)	Le
Greece	894	894	~~2126~~	0.04
Turkey	842	842	~~1891~~	-0.98
Gold Quarry	390	390	~~768~~	0.15
Aberfan, 1966	336	~~231~~	336	-0.03
Aberfan, 1944	357	357	~~556~~	-0.21
Aberfan, 1963	175	175	~~224~~	-0.07
Cilfynydd, 1939	392	~~271~~	392	0.01
Jupille, Belgium	593	593	~~871~~	-0.19
			AVG:	-0.18

Table 5: L_e as a function of volume (Golder, 1995)

The predictions from Formulas 2.1 and 2.2 proved to be quite accurate. The mobility of each of the 8 cases was determined by the empirical equations. Of the eight cases, only the 1966 Aberfan case and Cilfynydd were classified as highly mobile.

The predictions were accurate within 21% difference with respect to observed values of L_e in all cases except for the failure that occurred in Anatolia, Turkey, which was predicted to be 200% of its true value. Since so much volume was mobilized during the Turkey failure, one would have imagined that the runout would have been greater considering the formula only takes into account spreading ratio and volume. This inaccuracy can be explained by the low slope angle that was host to the slide. Had the failure slope been similar to some of the others discussed in this report, a much larger L_e most likely would have been displayed.

By taking the Turkey case as an outlier, the average prediction accuracy with respect to L_e is 4% and has a standard deviation of 13%. Even with the Turkey case, the formula is still accurate within 18% on average and has a standard deviation of 35%

For the cases presented in this report, Formulas 2.1 and 2.2 were successful in predicting L_e and showed tolerable variability.

4.1.2 Prediction of L_{toe} as a function of volume

The second prediction tool that is tested in this report is Formula 3.1 (Golder, 1995):

$$L_{toe} = (RR * c * V^n)^{1/2} \tag{3.1}$$

Formula 3.1 predicts the post-failure travel distance beyond the dump toe, L_{toe}, by taking volume; a spreading ratio, RR; and a constant, c, as inputs. As was done in Section 3.1.1, the spreading ratio was taken as the observed value of L_{toe}, (in this case L_{toe}) divided by the width of the slide, b. For predictions where spreading ratios are unknown, one must be assumed based on characteristics and setting of the waste dump.

The c value was taken to be 10, which is the lower limit for the typical range of this constant (10-20) for rock avalanches and debris flows.

In certain cases, there was no documentation of an observed L_{toe} value. For these cases, which are highlighted in purple in Table 6, an L_{toe} value was assumed to be equal to (L+Le)/2.

The results are shown in Table 6 below.

Event	Calculated Ltoe (m)	c	n	% Difference W.R.T. Ltoe
Greece	1470	10,00	0,67	-0,45
Turkey	1375	10,00	0,67	-1,68
Gold Quarry	321	10,00	0,67	-0,75
Aberfan, 1966	288	10,00	0,67	0,48
Aberfan, 1944	406	10,00	0,67	-0,13
Aberfan, 1963	176	10,00	0,67	0,23
Cilfynydd, 1939	280	10,00	0,67	0,39
Jupille, Belgium	356	10,00	0,67	0,21
			AVG:	-0,21

Table 6: L_{toe} as a function of volume (Golder, 1995)

The results made using Formula 3.1 varied. Half of the predictions made were overestimates while the other half were underestimates. When used for the coal mine database, the average accuracy of the predicted L_{toe} values was 17%, with respect to $L_{toe,}$ and with a standard deviation 23%. The average accuracy with respect to L_{toe} for the 8 cases in this report was overestimated by 21% and had a standard deviation of 73%. So, the Formula 3.1 showed decreased accuracy and increased variability in its results.

Six of the cases were predicted within 50% of the observed value, but the variability is greatly increased by the addition of the Turkey and Gold Quarry cases.

The Turkey case demonstrates the importance of properly selecting a spreading ratio for Formula 3.1. It can be seen that the activated volume for the Turkey case is half of the Greece case, yet because of the slight difference in their spreading ratios (0.72), a similar L_{toe} is predicted. If the Turkey case is taken as an outlier, the accuracy with respect to L_{toe} becomes an average of 0% and the standard deviation becomes 46%, which is a huge improvement.

The main problem with this formula is that it does not directly take into account the level of lateral confinement. Because of this, the predictions depend too much on volume and the constant, c. It also required very strong judgment and experience in selecting a proper spreading ratio, as mentioned above.

Overall, Formula 3.1 proved to be a good order of magnitude prediction, but its high variability makes it a poor candidate for reliable, accurate predictions. Future work could be done to improve the weighting of the inputs so that it more directly takes lateral confinement into account.

4.1.3 Prediction of L_{toe} as a function of height

The third prediction tool that is tested in this report is Formula 4 (Golder, 1995):

$$L_{toe} = [(c * R)^{\frac{1}{2}} * (e^{((h+G)/D)})^{1/N} + E]/F \qquad (4)$$

The variables are taken from and explained in detail in Golder (1995). C, R, G, N, E and F are independent variables and h is a dependant variable:

$$h = 73*\ln(V)-G \qquad (8)$$

The runout estimates and a comparison with the observed value are shown below in Table 7.

Event	Calculated Ltoe								Actual Ltoe	% Difference W.R.T.
	(m)	c	R	h	G	N	E	F	(m)	Ltoe
Greece	449	10	0,5	539	739	4	133	0,6917	1017	0,56
Turkey	408	10	0,5	488	739	4	133	0,6917	513	0,20
Gold Quarry	338	10	0,5	374	739	4	133	0,6917	183	-0,85
Aberfan, 1966	532	10	10,0	107	739	3	0	0,8958	550	0,03
Aberfan, 1944	264	10	0,5	167	739	4	133	0,6917	358	0,26
Aberfan, 1963	232	10	0,5	-6	739	4	133	0,6917	230	-0,01
Cilfynydd, 1939	525	10	10,0	104	739	3	0	0,8958	460	-0,14
Jupille, Belgium	253	10	0,5	118	739	4	133	0,6917	450	0,44
									AVG:	0,06

Table 7: L_{toe} as a function of height (Golder, 1995)

Six of cases were predicted within 45% and half of the cases were predicted within 20% of the observed values. When this formula was applied to the coal mine database, the formula overestimated the L_{toe} values by an average of 13% with respect to L_{toe} and had a standard deviation of 39%. For the eight new cases, Formula 4 overestimated the L_{toe} values by an average of 6% and had a standard deviation of 44%.

The accuracy and variability of the predictions remained very similar when applied to the eight new cases because the parameters taken were similar in both databases. It helps that all but two of the new cases are taken from coal mines. However, if Formula 4 took slope angle into account, the results may have differed since many of the new cases had a very different slope angle than the coal mine database cases.

Overall, Formula 4 proved to be quite accurate and showed moderate variability, as it did with its original database.

4.1.4 Prediction of Le as a function of volume

Formula 6 was perhaps the simplest of the formulas tested in this report as it only takes spreading ratio and volume into account:

$$L_e = R^{0.5} * 10^{0.95} * V^{0.28} \qquad (6)$$

The spreading ratio was chosen in a similar manner to the above sections.

The results are shown in Table 8 below.

Event	Calculated Le (m)	% Difference W.R.T. Le
Greece	1561	-0,67
Turkey	1440	-2,38
Gold Quarry	637	-0,38
Aberfan, 1966	338	-0,03
Aberfan 1944	536	-0,82
Aberfan 1963	245	-0,50
Cilfynydd, 1939	396	0,004
Jupille, Belgium	870	-1,175
	AVG:	-0,74

Table 8: L_e as a function of V (Golder, 1995)

Formula 6 predicted the Cilfynydd and 1966 Aberfan cases very accurately, although five of the eight cases were inaccurate by 50% or higher. One of the inaccurate predictions was the Jupille case, which is a prime example of the problems with excess travel distance as a measure of runout. As described earlier, this is because of the steepness of the path mantle and the substantial elevation loss. Because of this, the Jupille may have been able to be considered an outlier if it had been the only extreme inaccuracy. This was not the case however, as the Turkey case prediction was overestimated by 238%. The Jupille case also predicted such a high L_e because of its high R value, which was four times as high as most of the other R values. In this case, the formula places too much emphasis on the spreading ratio and not enough on volume.

For the eight cases, Formula 6 overestimated L_e on average by 74% with a standard deviation of 77%. It is concluded that this formula was unsuccessful because the values of its influencing factors differed greatly from the new cases to the cases from which the formula was derived.

4.1.5 Prediction of H/L as a function of volume

Formula 7 predicts was developed by Corominas (1996) and is used to predict H/L, which is the tangent of the fahrboschung, using volume and two coefficients, A and B, as inputs:

$$H/L = AV^{B} \qquad (7)$$

The A and B coefficients were taken from Hunter and Fell (2003) and depend on the magnitude of the activated volume.

There are two cases for which Formula 7 is tested: one case that doesn’t take lateral confinement into account (Table 9.1) and one that does (Table 9.2).

The calculated H/L values and their observed H/L values are shown in Tables 9.1 and 9.2 below.

Event	Confinement	Actual H/L	Volume V (m^3)	A	B	Calculated H/L	% Difference W.R.T. H/L
Greece	Unconfined	0,10	40.000.000	1,005	-0,1056	0,16	-0,58
Turkey	Unconfined	0,19	20.000.000	1,005	-0,1056	0,17	0,11
Gold Quarry	Unconfined	0,20	4.155.000	1,005	-0,1056	0,20	-0,03
Aberfan, 1966	Partly Confined	0,30	108.000	1,155	-0,1289	0,26	0,14
Aberfan, 1944	Confined	0,33	245.000	1,155	-0,1289	0,23	0,29
Aberfan, 1963	Confined	0,35	23.000	1,155	-0,1289	0,32	0,09
Cilfynydd, 1939	Confined	0,22	104.000	1,155	-0,1289	0,26	-0,17
Jupille, Belgium	Confined	0,92	125000	1,155	-0,1289	0,25	0,72
				all debris flows, <1.2x10^10		Avg:	0,07

Table 9.1: Equation for the prediction of H/L depending on confinement (Corominas, 1996)

Event	A	B	Calculated H/L	% Difference W.R.T. H/L
Greece	1,028	-0,1002	0,1779	-0,78
Turkey	1,028	-0,1002	0,1907	0,00
Gold Quarry	1,028	-0,1002	0,2233	-0,14
Aberfan, 1966	0,866	-1,095	0,0000	1,00
Aberfan, 1944	0,866	-1,095	0,0000	1,00
Aberfan, 1963	0,774	-0,0933	0,3032	0,13
Cilfynydd, 1939	0,866	-1,095	0,0000	1,00
Jupille, Belgium	0,866	-1,095	0,0000	1,00
			Avg:	0,40

unconfined, <1.2x10^10
confined, <1.2x10^10
confined, <10^5

Table 9.2: Equation for the prediction of H/L depending on confinement (Corominas, 1996)

The results for Formula 7 were unusual since the 'All slide' predictions ended up being more accurate than the predictions that took confinement into account. The average differences with respect to H/L were 7% and 40% respectively with standard deviations of 37% and 69%. For both cases, the predictions resulted in unconservative estimates of runout as the averages were underestimates of H/L.

Although the average for the second prediction, Table 9.2, was accurate to within 40% of H/L, there was a lot of variation as four of the eight cases were underestimated by 100% and one was overestimated by 78%. Therefore, these predictions should only be used as order of magnitude predictions and shouldn't be thought of as reliable assessments of risk for any given mine waste failure until further testing is done.

The 'All slides' predictions were the most accurate of the empirical formulas tested in this report. It showed similar variability to Formulas 2.1 and 2.2, but it produced greater accuracy with respect to the predicted value.

It is important to note that Formula 7 works well when calculating back-predictions, but it is much more difficult to provide reliable runout lengths since it outputs runout as a ratio of elevation loss to runout length. Because of this, the topography must be well studied and the case in question must be compared to similar mine waste dumps to determine common elevation losses.

4.2 Graphical predictions of H/L as a function of volume

This section includes the regression results of the coal mine data (Golder, 1995) and the subsequent addition of the new data, both of which are newly presented in this report. The regression comparisons presented in this section serve to show the regression results before and after the addition of the new data.

With a known or assumed volume of slide material, one can easily estimate the ratio of H/L using the following graphs. The graphs provide an alternate method of estimating runout and are often preferred when transparency and simplicity are of key importance.

The graphs are extremely useful when comparing cases with similar characteristics and setting, as can be seen in Figures 5.1, 6.1 and 7.1 below.

An alternate version of each graph can be seen in Appendix B.

4.2.1 Unconfined data

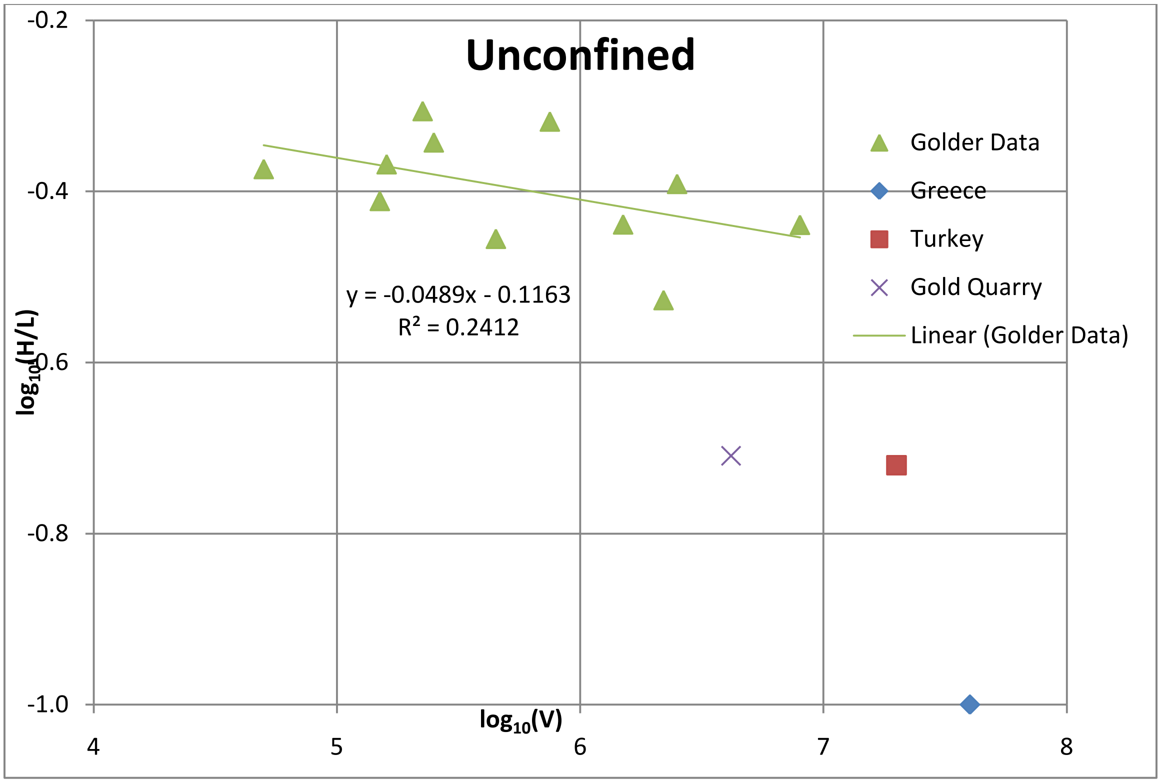

Figure 5.1: Regression results for the unconfined coal mine waste database

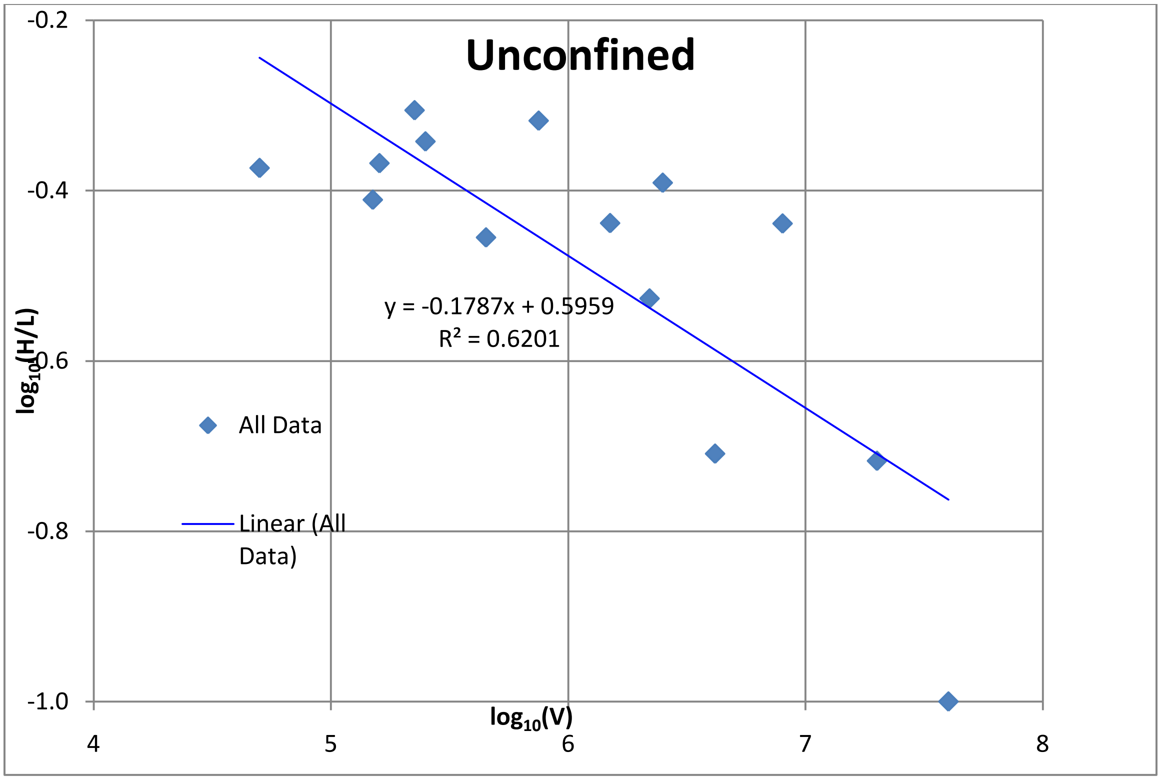

Figure 5.2: Regression results for the unconfined data in the coal mine waste and new databases

The addition of the three new cases to the data had large implications on the slope and correlation of the data. The standard deviation increased from 0.004 to 0.016 and the slope of the best fit line increased from -0.05 to -0.18. This change in slope is considerable and is due to the extreme mobility of the three new unconfined cases.

One very interesting change is that the coefficient of correlation, r^2, increased from 0.24 to 0.62. This signifies a strengthening of correlation with the addition of the new data. The new data actually served to improve the prediction ability of the graph despite the drastic change in slope and increase in the standard deviation.

4.2.2 Partly confined data

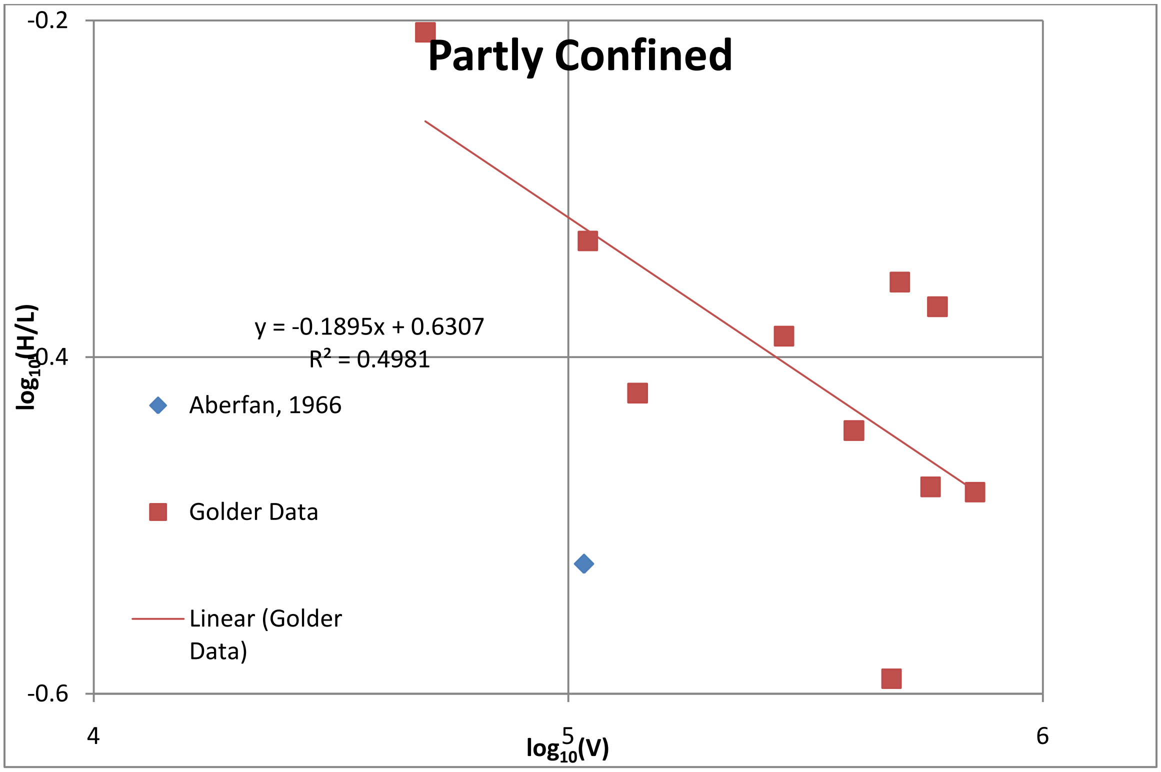

Figure 6.1: Regression results for the partly confined coal mine waste database

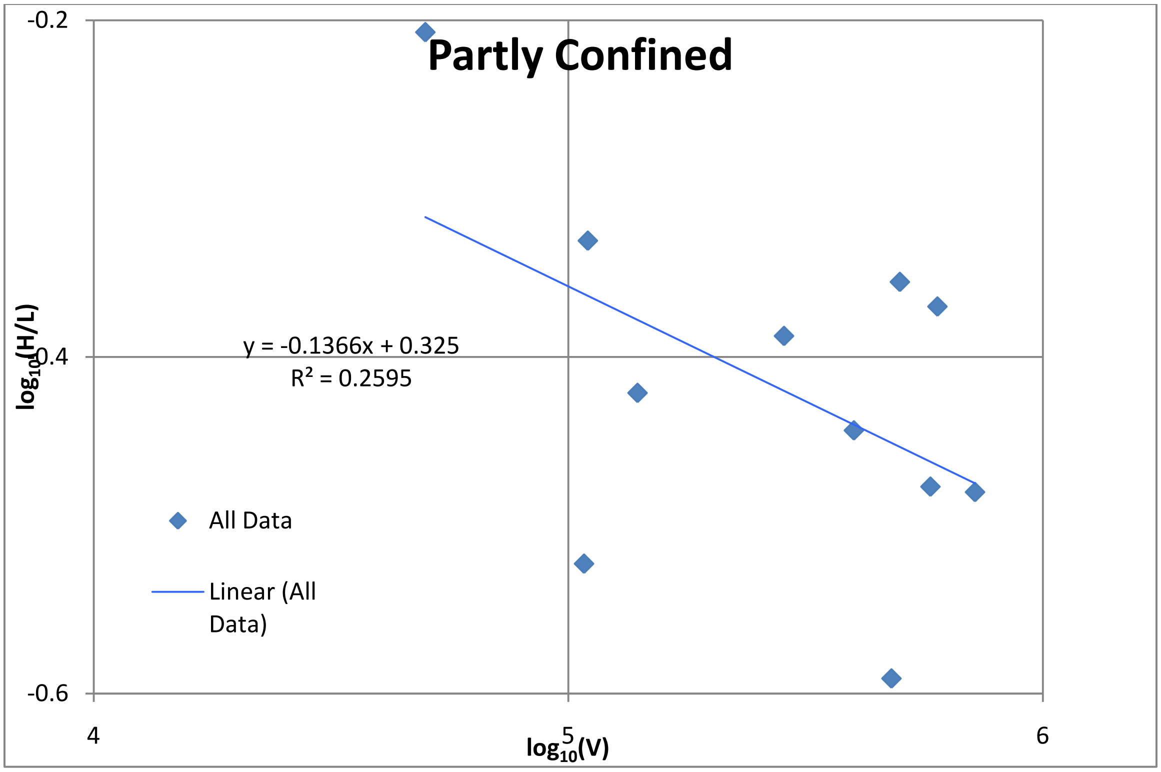

Figure 6.2: Regression results for the partly confined data in the coal mine waste and new databases

The partly confined Golder graph contained only ten points. With the addition of the 1966 Aberfan case, the slope decreased from -0.19 to -0.14 while the standard deviation increased from 0.006 to 0.009. The strength of the correlation also decreased as the coefficient of correlation, r^2, decreased from 0.50 to 0.26.

These statistical changes are quite strong considering the addition of the Aberfan case consists of less than 10% of the cases. This leads to the belief that for the Coal mine database, the Aberfan case is a clear outlier. A possible explanation for this lies in the above-mentioned definition of lateral confinement. Although the 1966 Aberfan case slightly fanned out towards the end of the slide, its confinement may have warranted it being grouped with the confined cases.

4.2.3 Confined data

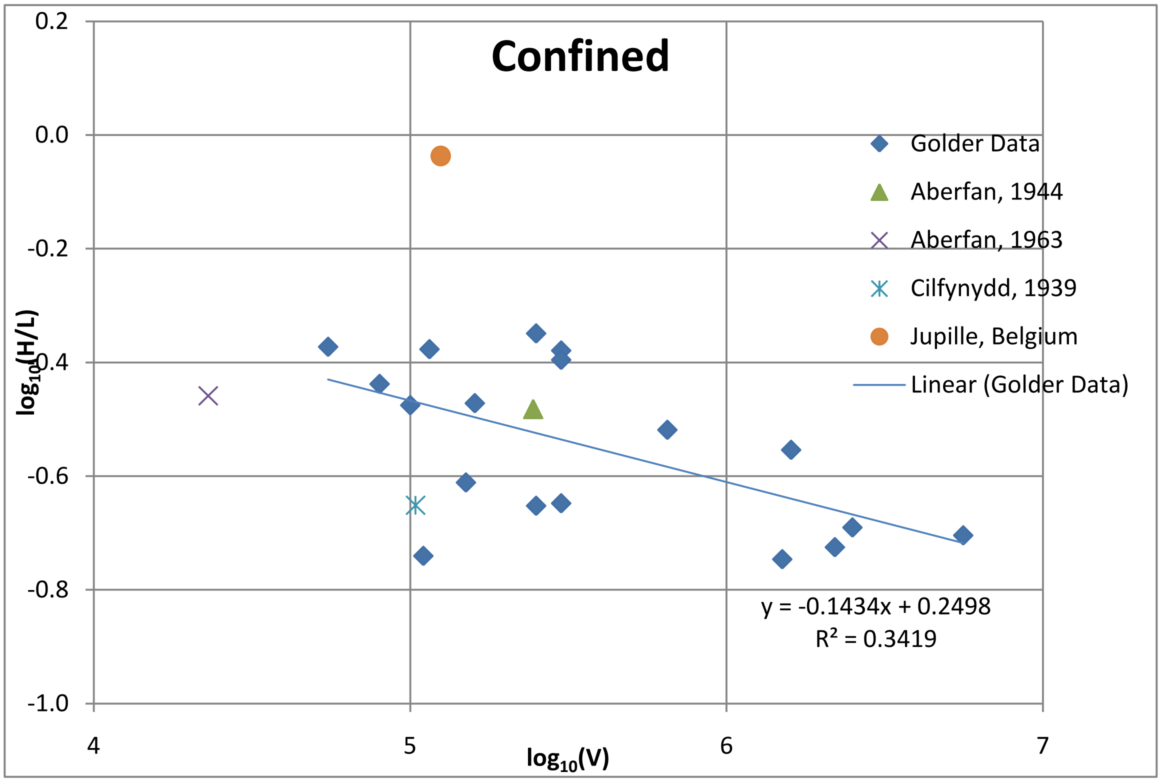

Figure 7.1: Regression results for the confined coal mine waste database

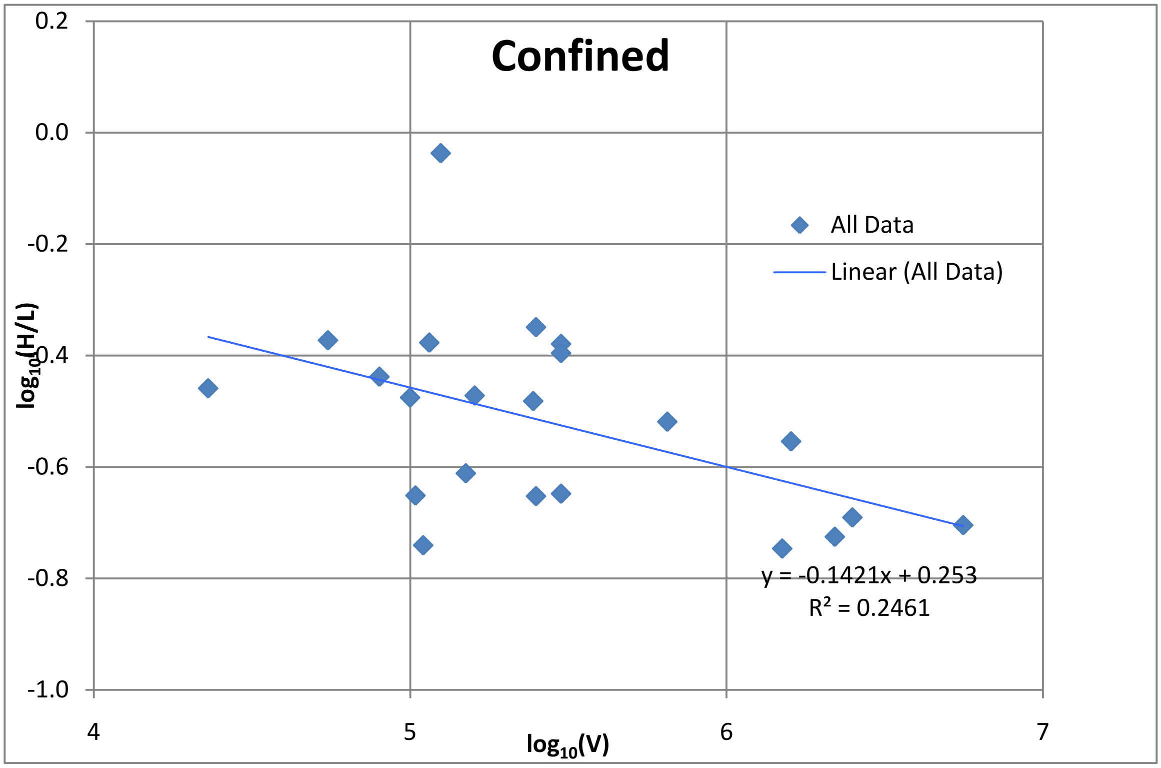

Figure 7.2: Regression results for the partly confined data in the coal mine waste and new databases

The addition of the four new confined cases had less of an effect on the data than the others. The standard deviation increased from 0.0145 to 0.0234, while the slope remained the same. The coefficient of correlation, r^2, decreased from 0.342 to 0.246. This indicates a decrease in the strength of correlation.

The statistical relationships between the new and old data would have been much stronger without the addition of the Jupille case, whose mobility was significantly higher considering its volume. This leads to the belief that the Jupille case is a clear outlier.

4.2.4 All data

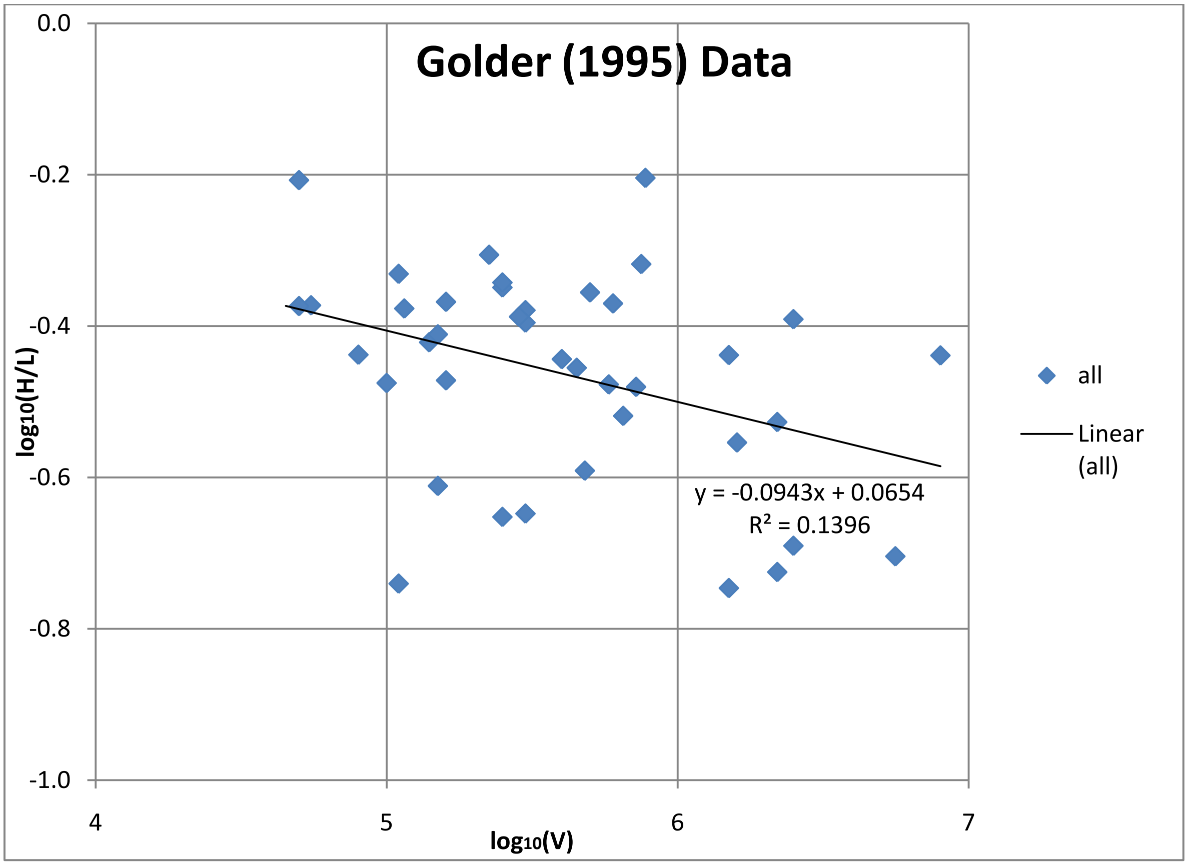

Figure 8.1: Regression results for coal mine waste database

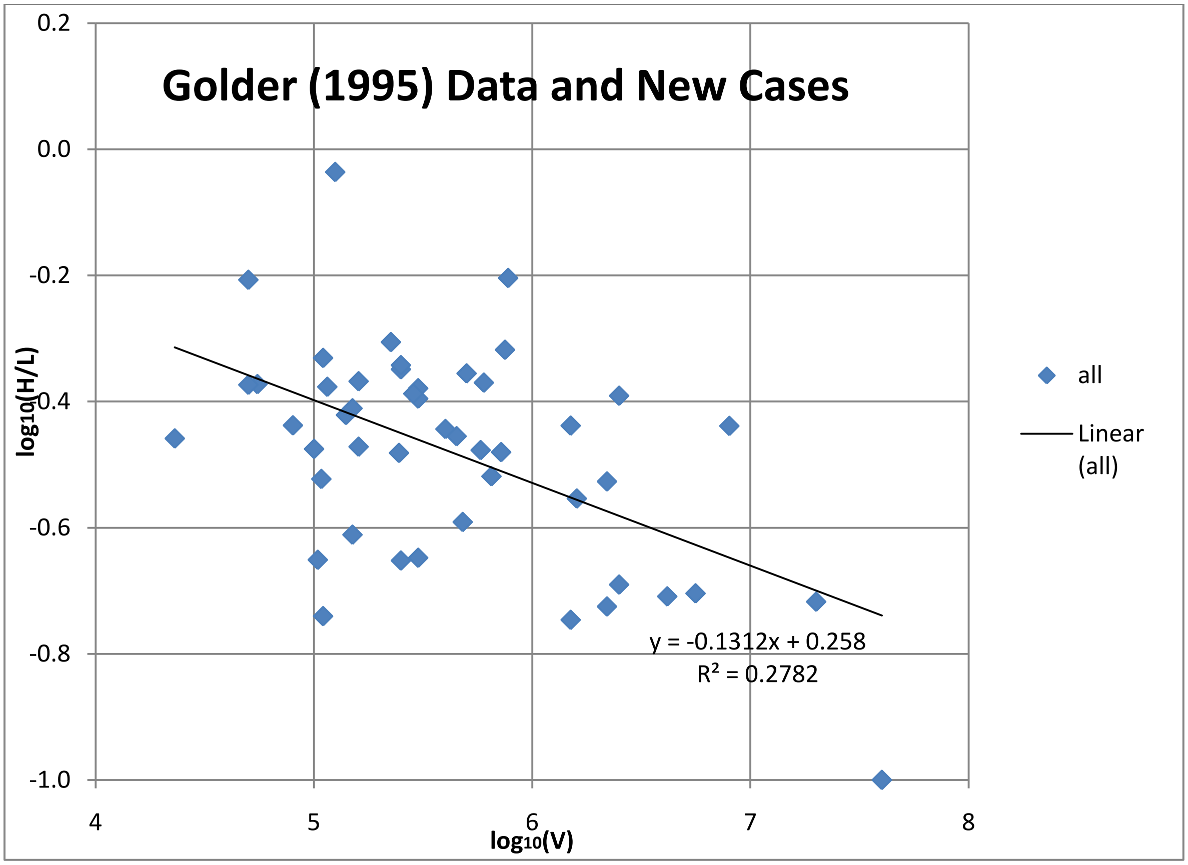

Figure 8.2: Regression results for coal mine waste database and new cases

The addition of all the new data resulted in an increase in slope, standard deviation and coefficient of correlation for the best fit line. Although the Figure 8.2 does not offer an effective prediction of runout (compared to Figures 5, 6, 7), they do serve to show the difference between the coal mine data and the new data.

These graphs further support the idea that runout prediction tools should be specific to the cases in question. Since the conditions of the waste dumps in the BC Rocky Mountains were so different from the new cases, one would expect there to be varying results, and these graphs act as proof of this.

4.2.5 All confinement levels

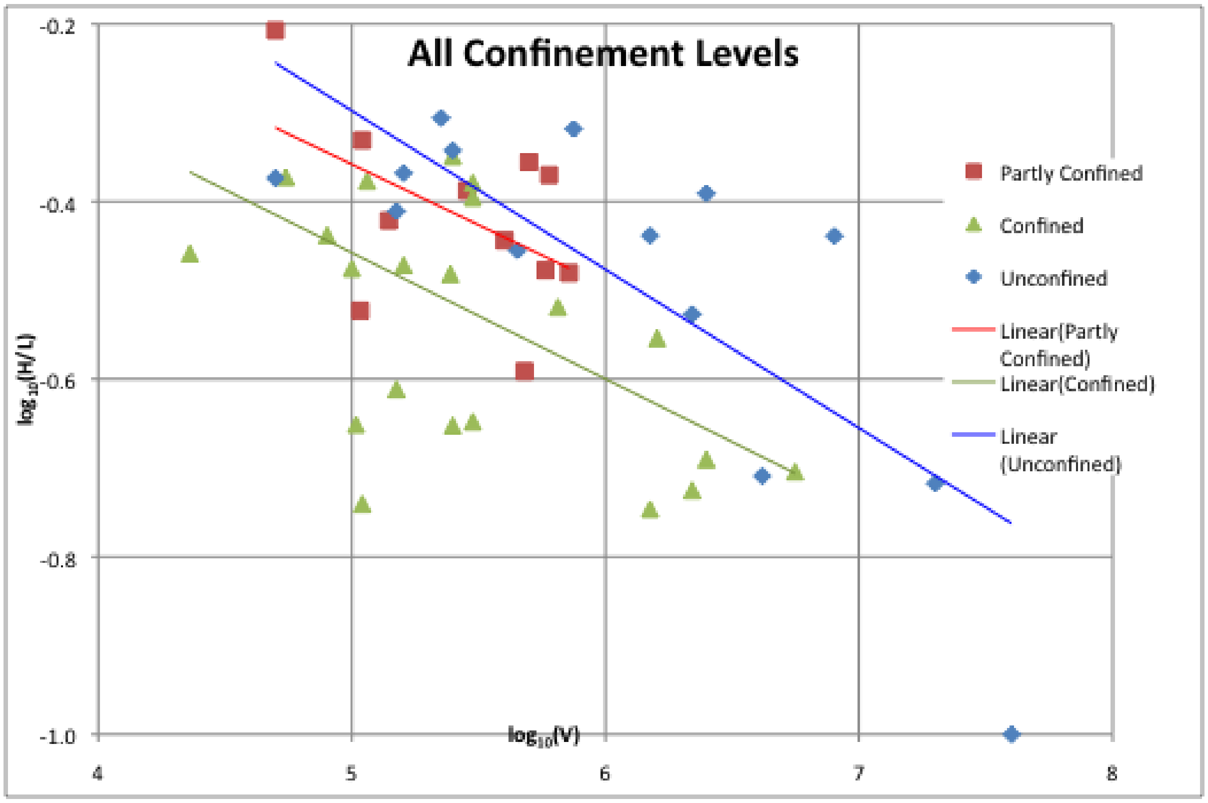

Figure 9: All confinement levels

Figure 9 effectively displays the well known relationship in the relative mobility of the different confinement levels. It incorporates data from the Golder cases and the new case. It is interesting to note that without the Greece waste dump; all the best fit slopes would be very similar.

4.3 Runout exceedence probability

This section consists of a volume- fahrböschung method that was originally applied to rock avalanches and is based on regression results presented by Li (1983). The plots show the change in predicted exceedence probability with distance from the source, where each line represents a given magnitude. Once the magnitude of volume and fahrböschung for a mine waste dump is known or assumed, the associated probability of exceeding the runout distance can be read off the graph.

Each confinement level is accompanied by two figures that are used to contrast the data from Golder (1995) and the new cases.

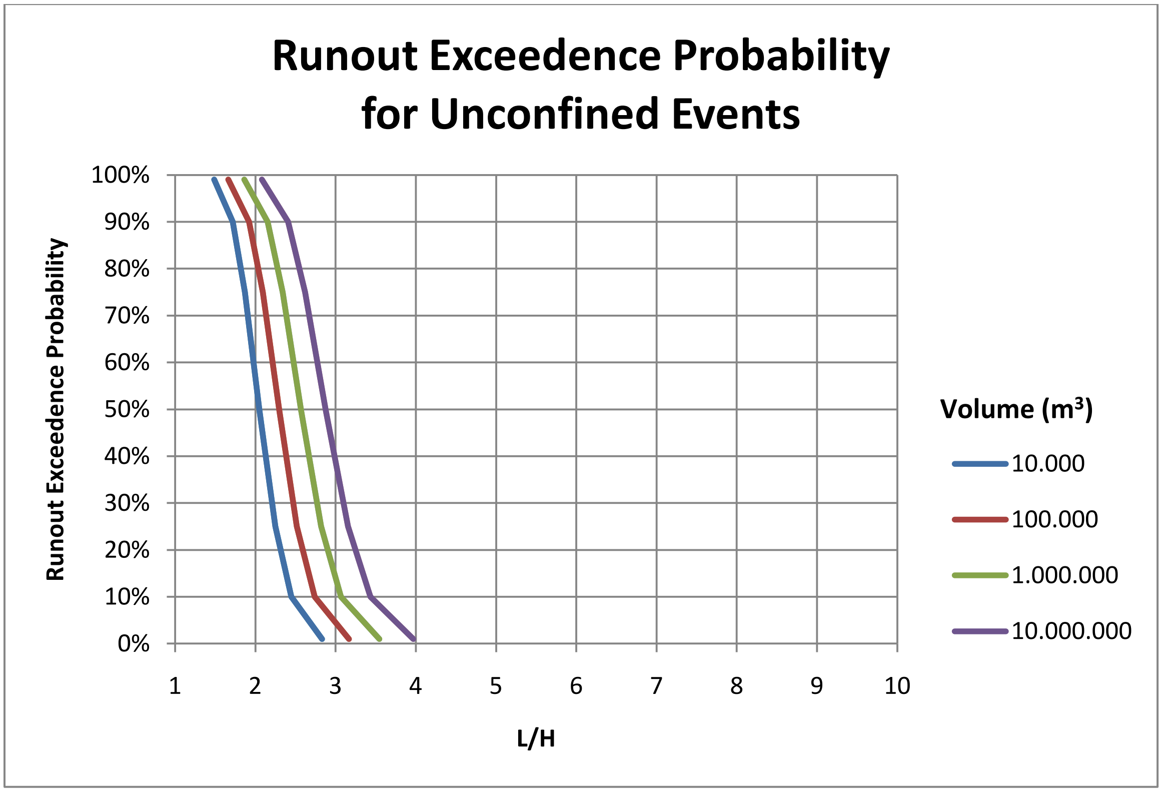

Figure 10.1: Golder data (1995) - unconfined

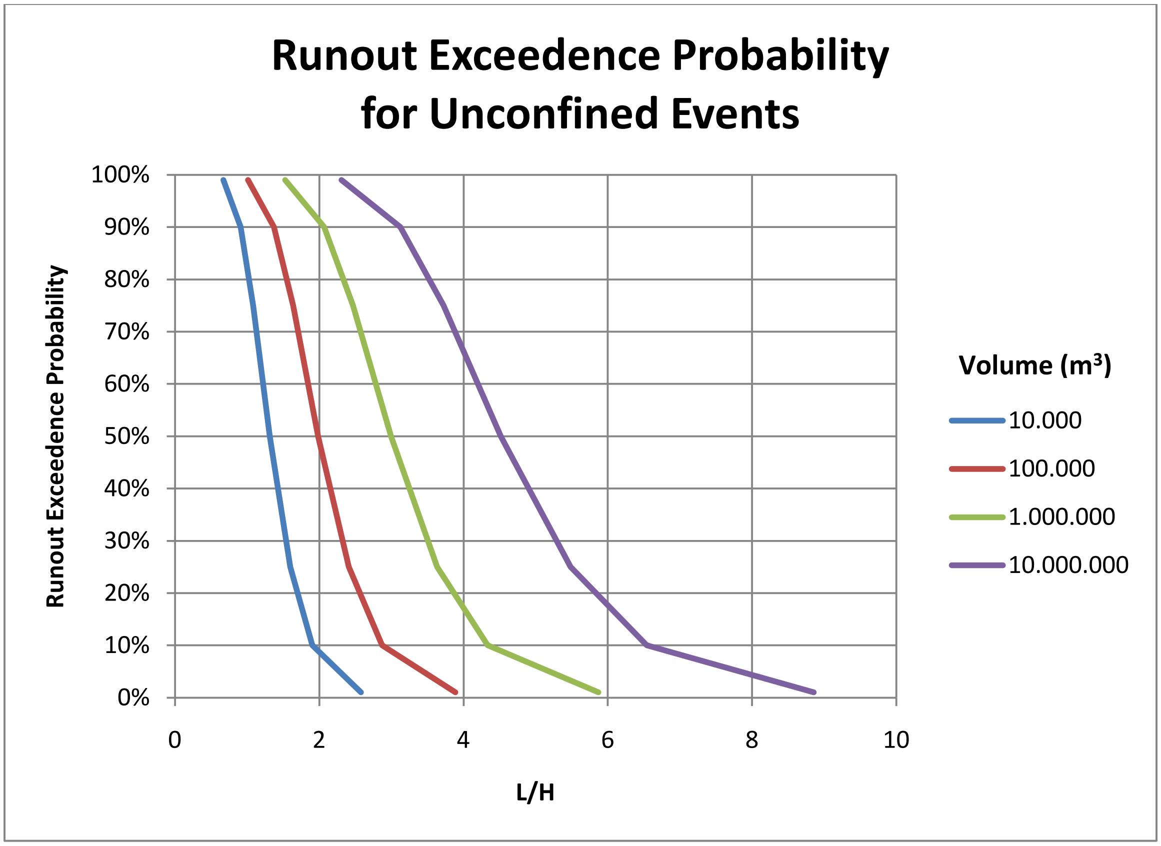

Figure 10.2: Golder data (1995) and new data – unconfined

4.3.1 Unconfined data

The addition of the new unconfined data had a large effect on the confidence bounds for the prediction. Figures 10.1 and 10.2 show the 10^6 and 10^7 magnitude prediction lines drastically shifted forward from 3.5 and 4 to 6 and 9, respectively. This graph shows how much more mobile the new unconfined data was compared to the unconfined Golder cases.

According to Figure 10.2, there was a very low probability (near 1%) of the Greece case reaching the travel distance that was recorded. The Turkey case had a probability of approximately 45%, while the Gold Quarry case had a probability of approximately 20%.

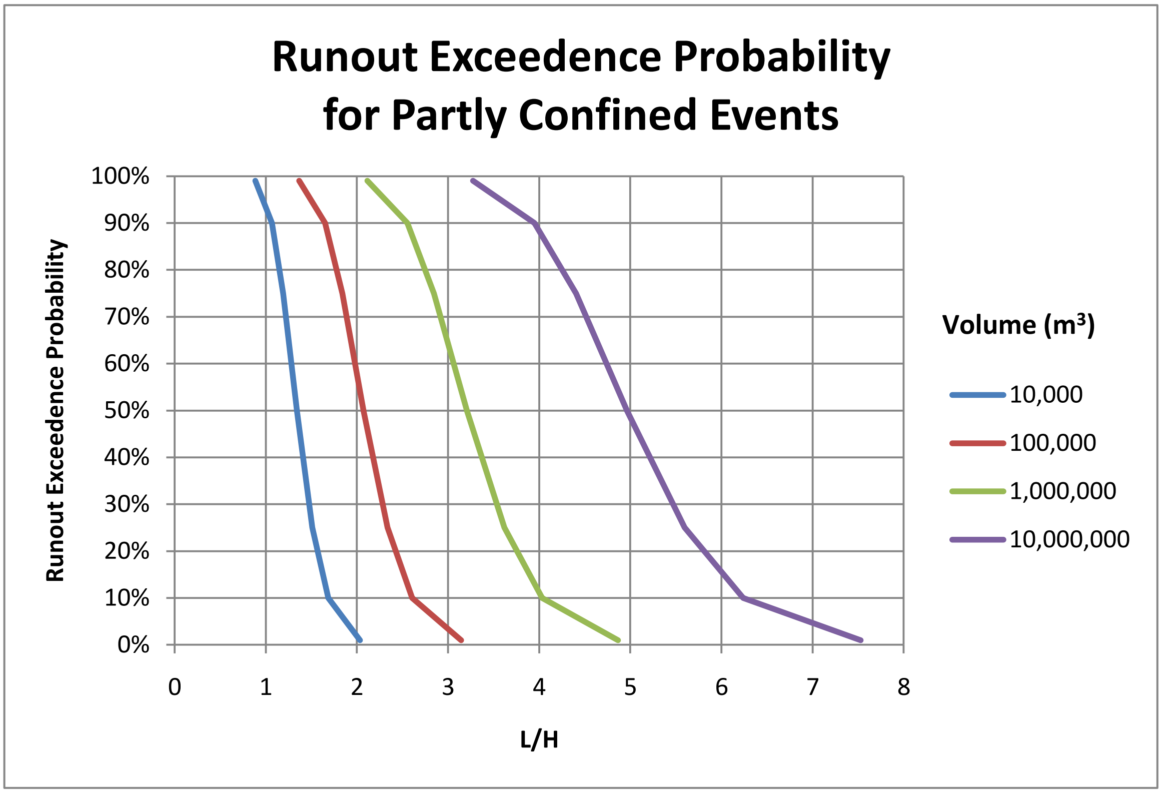

Figure 11.1: Golder data (1995) – partly confined

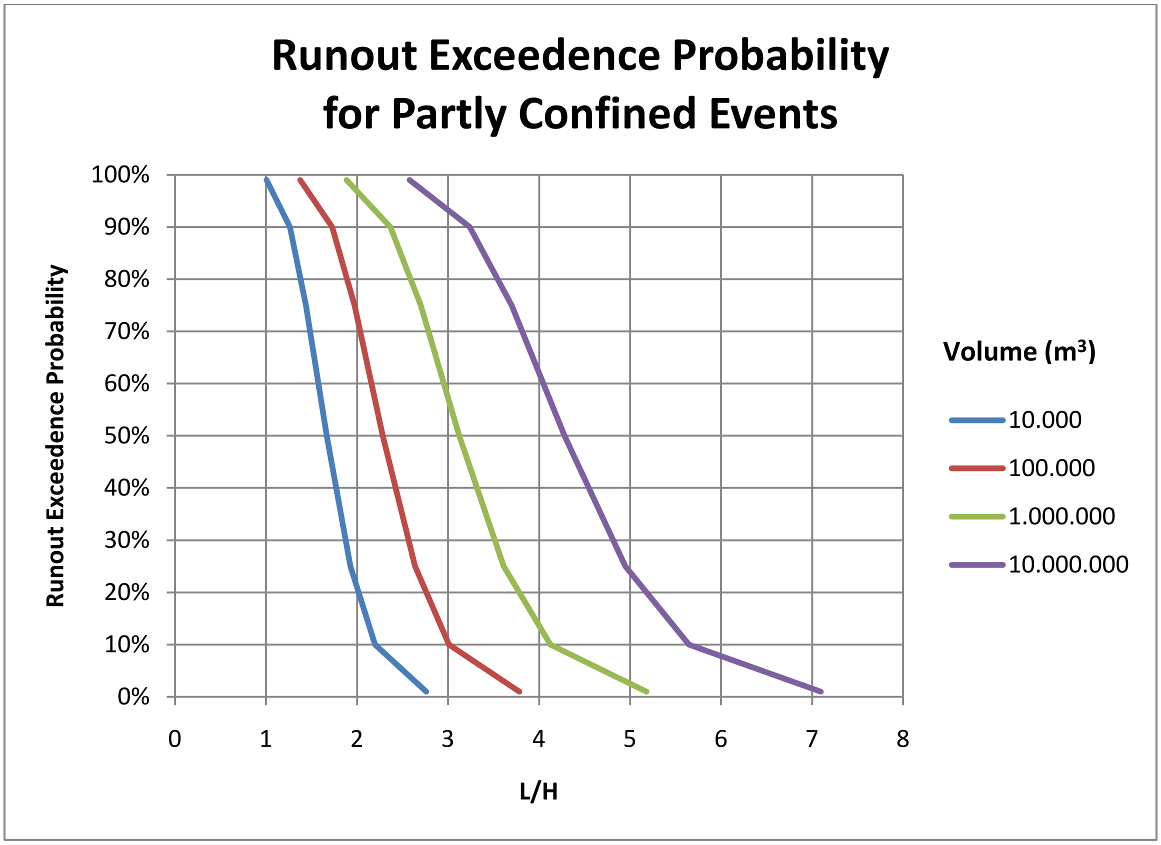

Figure 11.2: Golder data (1995) and new data-partly confined

4.3.2 Partly confined data

The addition of the new partly confined data did not have a significant effect on the confidence bounds, but this is partly because there was only one case added. With the addition of the 1966 Aberfan case, the 10^6 line slightly decreased its mobility probability and the 10^7 line slightly increased its mobility probability (As seen in Figures 11.1 and 11.2).

Based on the 1966 Aberfan volume, there was less than a 1% chance of it reaching the runout distance that it did. If it had been classified as a confined slide, then there would have been a 40% chance of reaching the runout distance (according to Figure 12.1).

4.3.3 Confined data

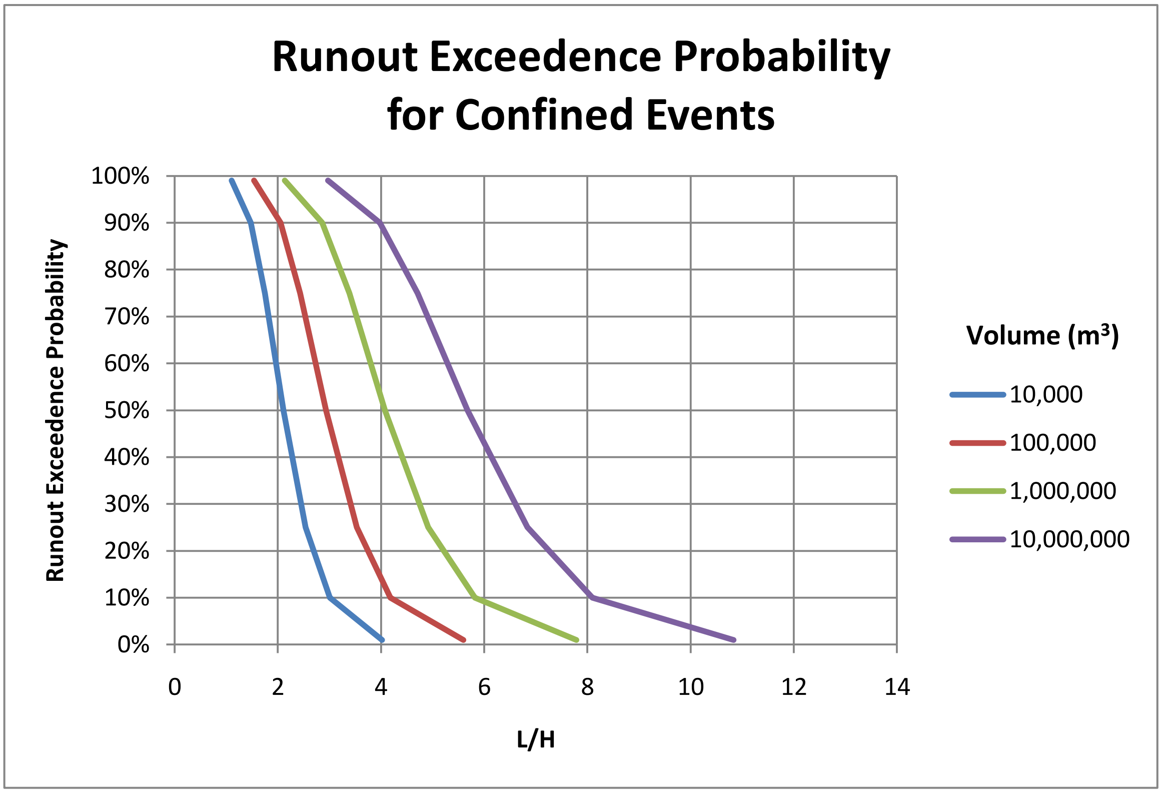

Figure 12.1: Golder data (1995) - confined

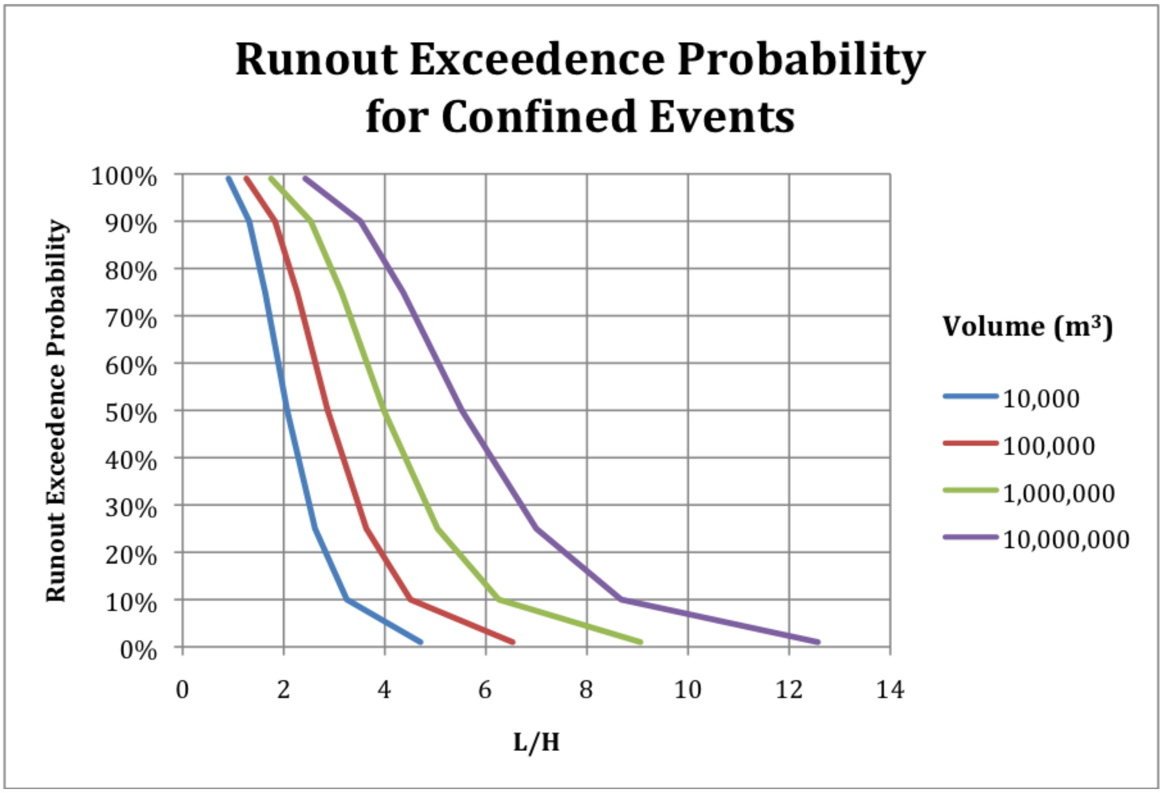

Figure 12.2: Golder data (1995) and new data - confined

The addition of the confined data had a moderate effect on the graphs by increasing the confidence bounds for all magnitudes (as seen in Figure 12.1 and 12.2).

Based on Figure 12.2, the approximate probabilities of Aberfan (1944), Aberfan (1963) and Cilfynydd in reaching there runout distances based on their volume and elevation loss were 40%, 20% and 10% respectively. Perhaps the most interesting point to note is that Figure 12.2 predicted that there was a 99% chance that Jupille case would reach its L/H ratio. This observation is opposite to the empirical predictions of the Jupille case, which suggested that Jupille was an outlier. This is one of the problems with displaying runout as a ratio of distance travel to elevation loss: since the Jupille slide measured such a large elevation loss, the ratio was diminished and thus the probability of the slide reaching a large runout distance increased.

5. CONCLUSIONS AND RECOMMENDATIONS

Mine waste failures are complex processes with significant variability. Since there are so many factors affecting the runout of a slide, empirical models tend to be oversimplifications. The models are then further subjected to interpretation and measurement error which increase the uncertainty. Furthermore, the predictions can be very misleading when they are not applied to cases within a similar setting and conditions. Because of these facts, empirical formulas should be accompanied by graphical and analytical prediction tools and should never be used without significant engineering judgment.

In this report, five empirical tools and two graphical tools were used to evaluate runout distances in an attempt to test the accuracy of the tools outside their original database. The tools were applied to the eight new mine waste dump failures, and in some instances, the waste failures from the Golder database (1995).

The results of the predictions made using the empirical tools varied greatly. Formulas 2.1, 2.2, 4 and 7.1 provided accurate predictions of runout with similar variability to that of the original back-analyses. Formulas 3.1 and 6 were less accurate in predicting the runout of the new cases and had significant variation. It is believed that this is due mainly to the fact that the controlling factors of the new and old databases were sufficiently different because of their different mine dump characteristics and setting.

Generally, empirical runout tools should be used on similar cases to those that were used to develop the tools. When the tools are applied to cases outside their original database, the results are less dependable. Furthermore, considerable judgment should be used when selecting model parameters and interpreting results.

The graphical tools, which present the runout predictions in terms of probabilities and best guesses, provide another method of displaying runout predictions. In this report, they proved to be useful in supporting the empirical formulas and in providing a simple and informative deliverable; however, they too showed some variability and should be accompanied by other tools.

No matter how accurate the runout prediction tools may be at assessing the risk of a waste dump, they should never replace the need for proper mine waste monitoring practice. As was seen in almost all of the cases presented, the failures were preceded by substantial horizontal and/or vertical deformation of the dump crest. Through the use of simple wireline extensometers, the failures may have been successfully anticipated.

ACKNOWLEDGEMENTS

I am deeply thankful to my thesis advisor, Scott McDougall, for all of his support, guidance and patience from the initial to the final stages, without which the realization of this project would not have been possible.

I would also like to thank Oldrich Hungr for his direction and previous work which established the foundation for this report.

Gabriel Srour

REFERENCES

Abele, G. 1974. Bergsturze in den Alpen. Wissen schaft liche Alpen vere in shefte, Number 25, Munich, (In German).

Bishop, A.W., Hutchinson, J.N., Penman, A.D.M. & Evans, H.E., 1969. Geotechnical investigations into the causes and circumstances of the disaster of 21st October 1966. A selection of technical reports submitted to the Aberfan Tribunal, Welsh Office. London: H.M.S.O.

Bishop, A.W. 1973. The stability of tips and spoil heaps. Quarterly Journal of Engineering Geology, 6, 335-376.

Corominas, J. 1996. The angle of reach as a mobility index for small and large landslides. Canadian Geotechnical Journal, 33: 260-271.

Dawson, R.F., Morgenstern, N.R., Stokes, A.W. 1998. Liquefaction flowslides in Rocky Mountain coal mine waste dumps. Canadian Geotechnical Journal, 35: 328-343.

Golder Associates Limited. 1995. Mined Rock and overburden piles: runout characteristics of debris from dump failures in mountainous terrain. Stage 2: analysis, modeling and prediction. Interim Report, Report No. 932-1493. Prepared in association with O. Hungr Geotechnical Research Ltd. British Columbia Mine Waste Rock Pile Research Committee and CANMET. Contract No. 23440-0-9198-X86

Harlan, J.B., Harris, D. A., Mallette, P. M., Norby, J. W., Rota, J. C., & Sagar, J. J. 1999. Geology and Mineralization of the Maggie Creek District. Gold Deposits of the Carlin Trend. Nevada Bureau of Mines and Geology Bulletin, 111: 115-142.

Heim, A. 1932. Bergstruz and Menschenleben. Fretz and WasmuthVerlag, Zurich, Switzerland.

Hsu, K.J. 1975. Catastrophic debris streams (Sturzstroms) generated by rockfalls. Geological Society of America Bulletin, v. 86, pp 129-140, January 1975.

Hungr, O. 1990. Mobility of rock avalanches: Tsukuba, Japan. Reports of the National Research Institute for Earth Sciences and Disaster Prevention, v. 46, p. 11-20.

Hungr, O. 1995. A model for the runout analysis of rapid flow slides, debris flows and avalanches. Canadian Geotechnical Journal, 32(4): 610-623.

Hungr, O., Evans, S.G., Bovis, M.J., Hutchinson, J.N., 2001. A Review of the classification of landslides of the flow type: Environmental and Engineering Geoscience, v. VII, p. 221–238.

Hunter, G. and Fell, R. 2003. Travel distance angle for ‘rapid’ landslides in constructed and natural slopes. Canadian Geotechnical Journal, 40: 1123-1141.

Hutchinson, J.N. 1986. A sliding-consolidation model for flow slides. Canadian Geotechnical Journal, 23: 11-126

Hutchinson, J.N., 1992b, Flow slides from natural slopes and waste tips, in Proceedings, 3rd National Symposium on Slopes and Landslides, La Coruna, Spain, pp. 827-841.

Li, T. 1983. A mathematical model for predicting the extent of a major rockfall. Zeitschrift fur Feomorphologie, 27: 473-482.

Locat, J., and Leroueil, S. 1997. Landslide stages and risk assessment issues in sensitive clays and other soft sediments. In Proceedings of the International Workshop on Landslide Risk Assessment, Hawaii, Edited by D. Cruden and R. Fell. A.A. Balkema Rotterdam, The Netherlands. pp. 261-270

Mclemore, V.T., Donahue. K.M., Walsh, P., Tachie-Menson, S., Phillips, E.H., Guitierrez, L.A.F., and Shannon, H.R.. 2005. Trench Sampling of the Molycorp Goathill North Rock piles, Questa Rock Pile Stability Study, New Mexico: National Meeting of the American Society of Mining and Reclamation, Breckenridge, Colorado, June, CD-ROM, 26. http://geoinfo.nmt.edu/staff/mclemore/Molycorppapers.html

Ministry of Energy, Mines and Petroleum Resources (MEMPR). 1992. "Review and Evaluation of Failures"; Prepared by Scott Broughton for the British Columbia Mine Dump Committee, March.

Melosh, H.J. 1979. Acoustic Fluidization: A New Geologic Process? Journal of Geophysical Research, Vol. 84, pp. 7513-7520.

Nichols, R.R. 1987. Rock Segregation in waste dumps; In: Flow-through rock drains: Proceedings of the International symposium convened at the Inn of the South, Cranbrook, B.C., September 8-11, 1986.

Nicoletti, P.G. and Sorriso-Valvo, M. 1991. Geomorphic controls of the shape and mobility of rock avalanches. Geological Society of American Bulletin, 103: 1365-1373.

Regnier, J. 1960. Cenozoic geology in the vicinity of Carlin, Nevada. Geological Society of America Bulletin, 71(8): 1189-1210.

Robertson, A., and Skermer, N.A. 1988. Design Considerations for the Long Term Stability of Mine Wastes, in First International Environmental Workshop, Darwin.

Sheets, R. J. & Bates, E. E. 2008. Gold Quarry North Waste Rock Facility Slide Investigation and Stabilization. Tailings and Mine Waste, pp. 19-22, 2008

Scheiddeger, A.E., 1973. On the Prediction of the Reach and Velocity of Catastrophic Landslides. Rock Mechanism Vol. 5, pp. 231-236, 1973

Siddle, H.J., Wright, M.D., and Hutchinson, J.N. 1996. Rapid failures of colliery spoil heaps in the South Whales coalfield. Quarterly Journal of Engineering Geology, 29: 103-132.

Steiakakis, E., Kavouridis, K., and Monopolis, D., 2008. Large scale failure of the external waste dump at the “South Field” lignite mine, Northern Greece. Engineering Geology, V. 104,23 March 2009, Pages 269-279.

Ulusay, K., Kasmer, O., Gokceoglu, C. 2005. Spoil pile instabilities with reference to a strip coal mine in Turkey: mechanisms and assessment of deformations. Environmental Geology (2006) 49: 570–585

Varnes, D.J., 1978. Slope movement types and processes. Landslides, Analysis and Control, Transportation Res. Board Spec. Report, Schuster, R.L. & Krizek, R.J. Ed., pp. 11-33

Zahl, E. G., Biggs, F., Boldt, C. M. K., Connolly, R. E., Gertsch, L., and Lambeth, R.H., 1992, Waste Disposal and Contaminant Control, in Hartman, H. L., ed., SME Mining Engineering Handbook: Littleton, CO, Society for Mining, Metallurgy and Exploration Inc., p. 1170-1180.

APPENDIX A

i.Aberfan

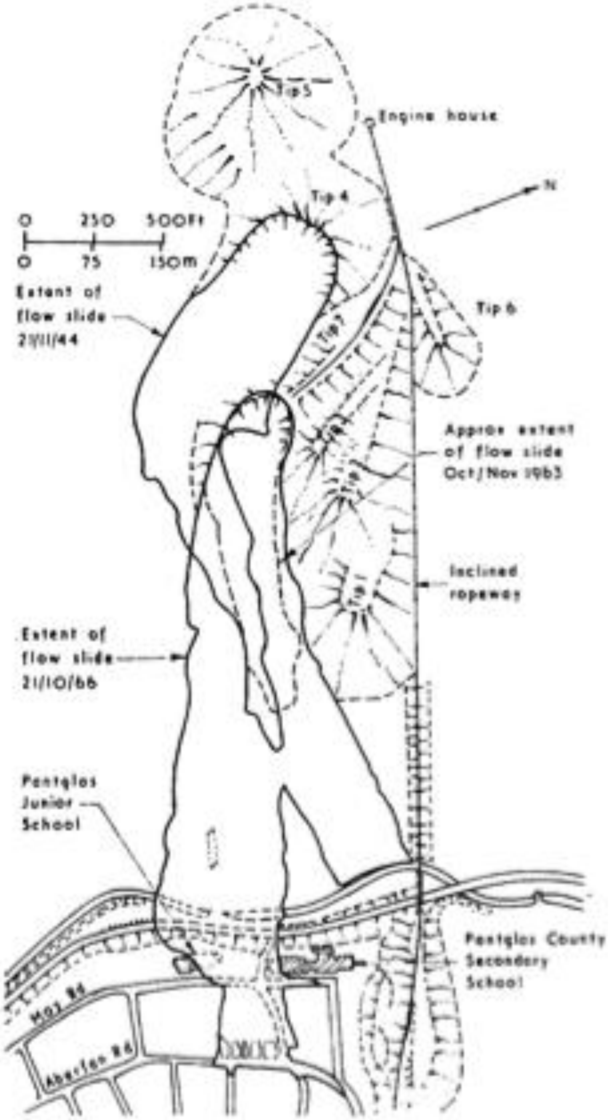
Tip 5
Engine house
Tip 4
N
0 250 500Ft
0 75 150m
Extent of flow slide 21/11/44
Tip 6
Tip 7
Approx extent of flow slide Oct/Nov 1963
Inclined ropeway
Extent of flow slide 21/10/66
Pantglas Junior School
Pantglas County Secondary School
Moy Rd
Aberfan Rd

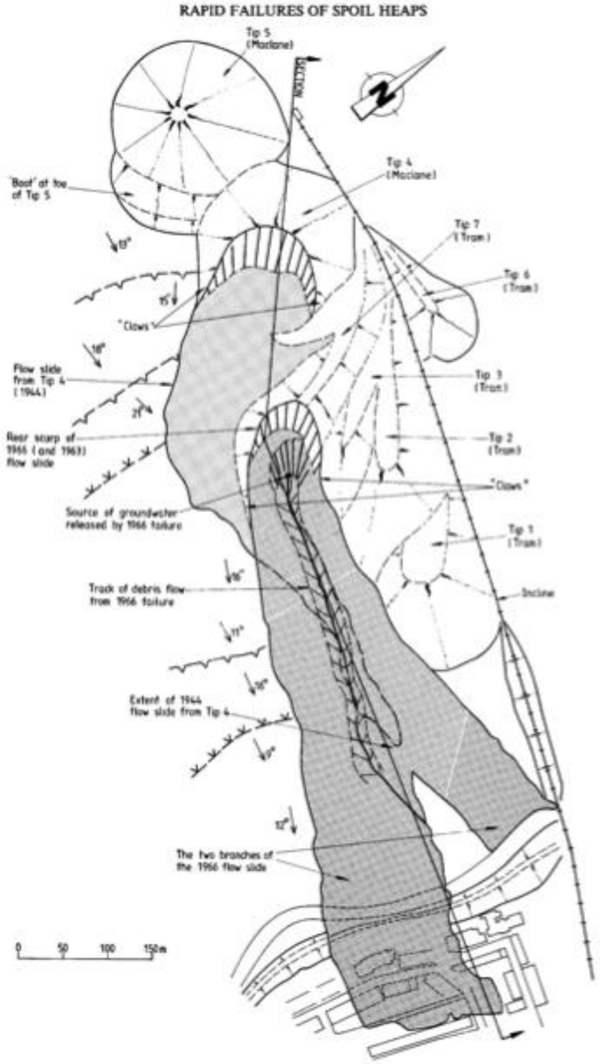
RAPID FAILURES OF SPOIL HEAPS
Tip 5 (Maclane)
SECTION
N
'Boot' at toe of Tip 5
Tip 4 (Maclane)
Tip 7 (Tram)
Tip 6 (Tram)
13°
15°
"Claws"
18°
Flow slide from Tip 4 (1944)
Tip 3 (Tram)
21°
Rear scarp of 1966 (and 1963) flow slide
Tip 2 (Tram)
"Claws"
Source of groundwater released by 1966 failure
Tip 1 (Tram)
16°
Track of debris flow from 1966 failure
Incline
11°
10°
Extent of 1944 flow slide from Tip 4
9°
12°
The two branches of the 1966 flow slide
0 50 100 150m

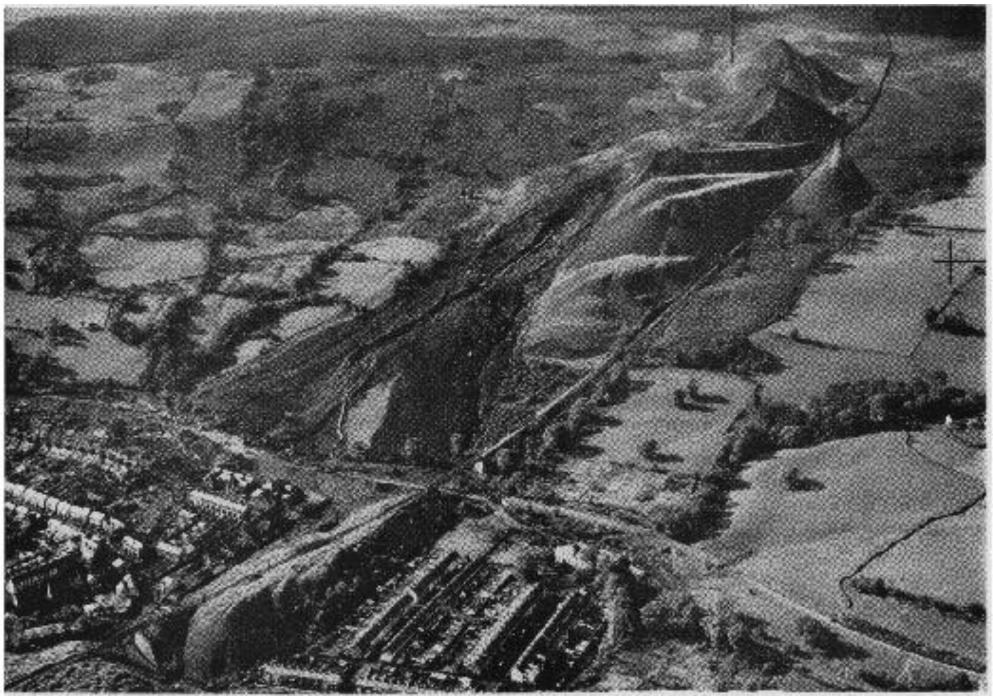

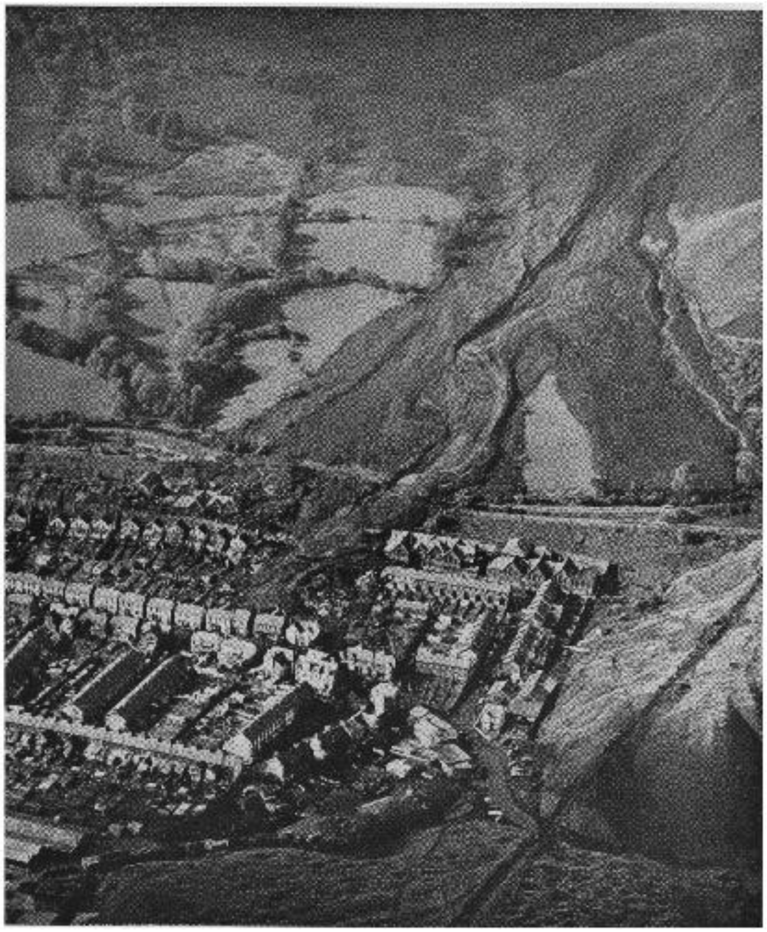

ii. Cilfynydd

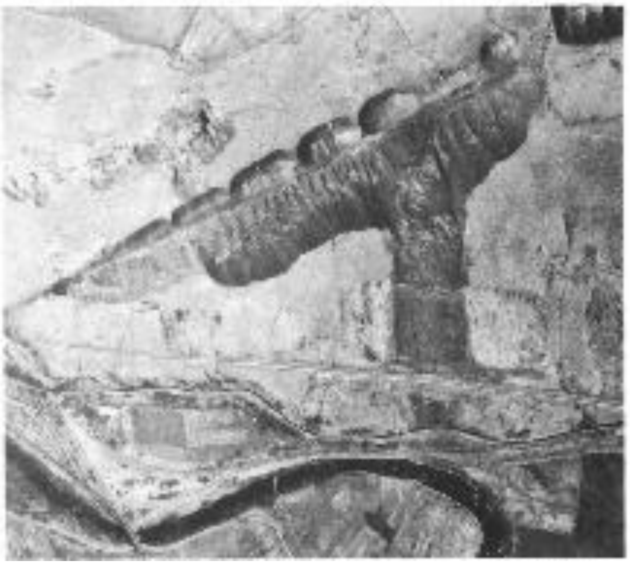

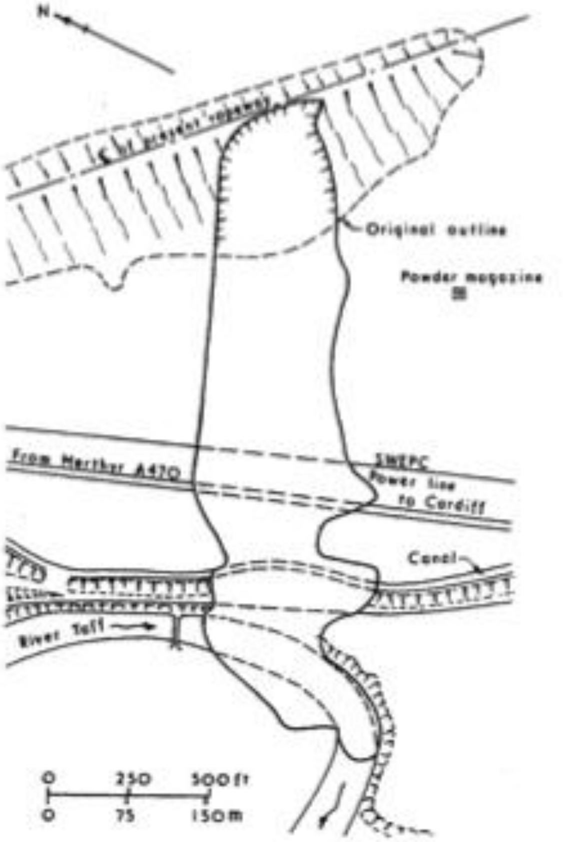
N
Original outline
Powder magazine
From Merthyr A470
SWEPC
Power line
to Cardiff
Canal
River Taff
0
250
500 ft
0
75
150 m

iii. Jupille

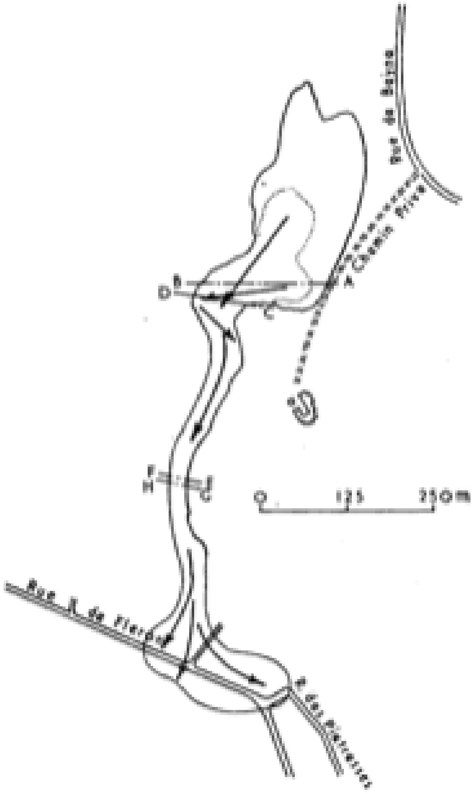
Rue de Bayne
Chemin Privé
A
B
C
D
E
F
G
H
0
125
250m

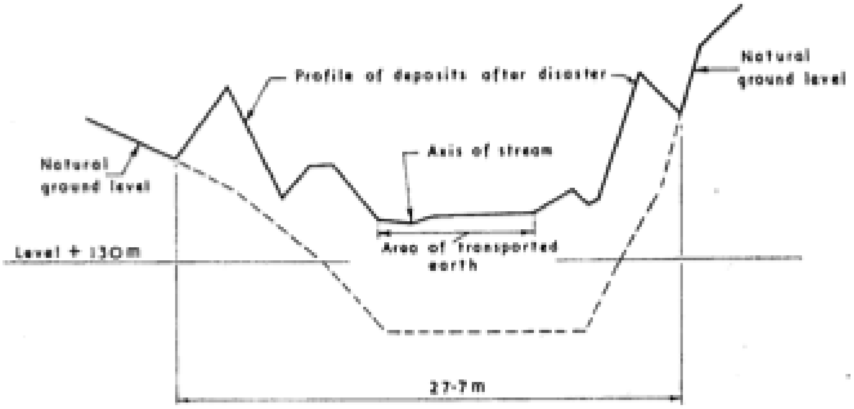
Profile of deposits after disaster
Natural ground level
Natural ground level
Axis of stream
Area of transported earth
Level + 130m
27·7m

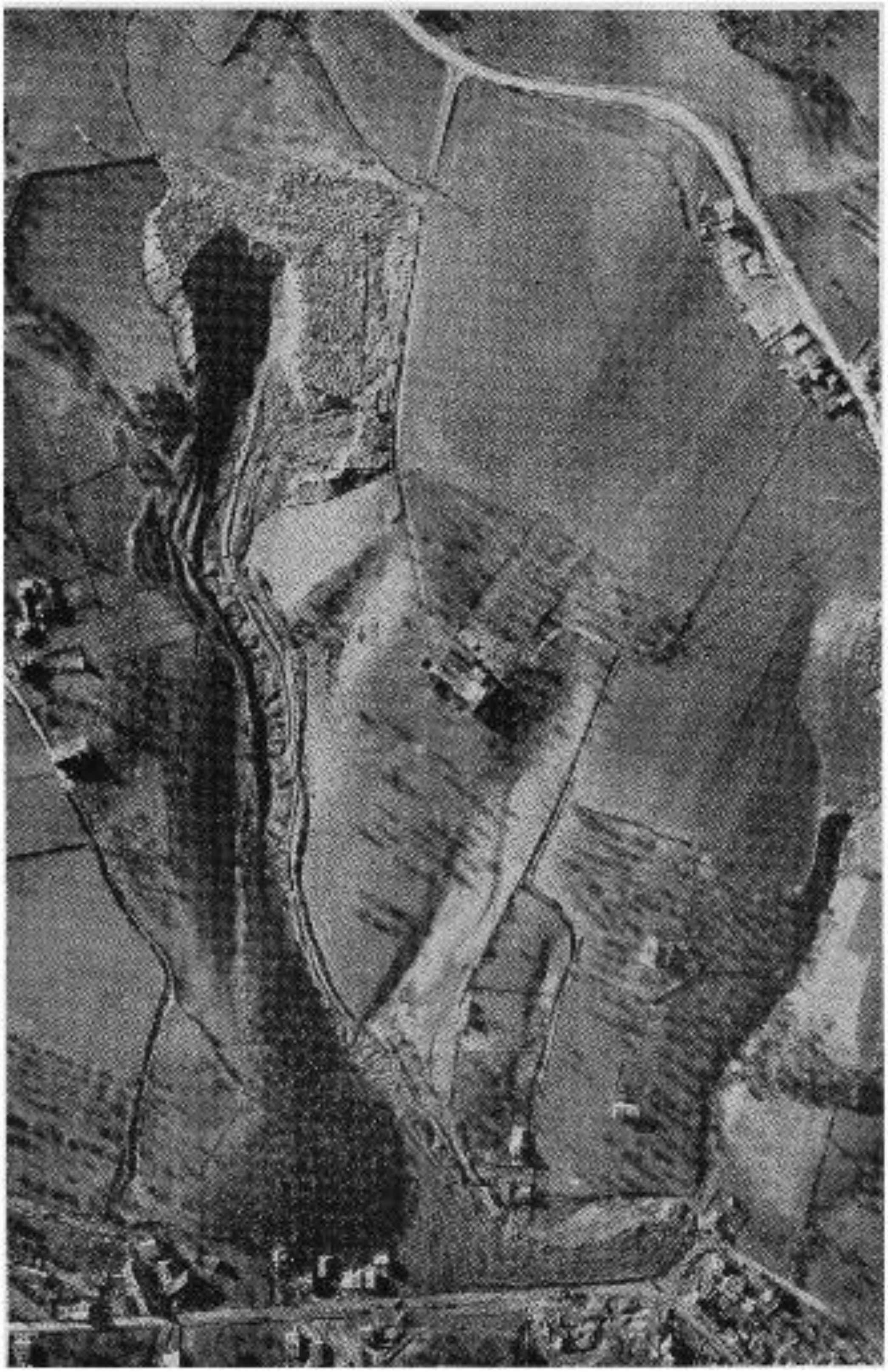

iv. Gold Quarry

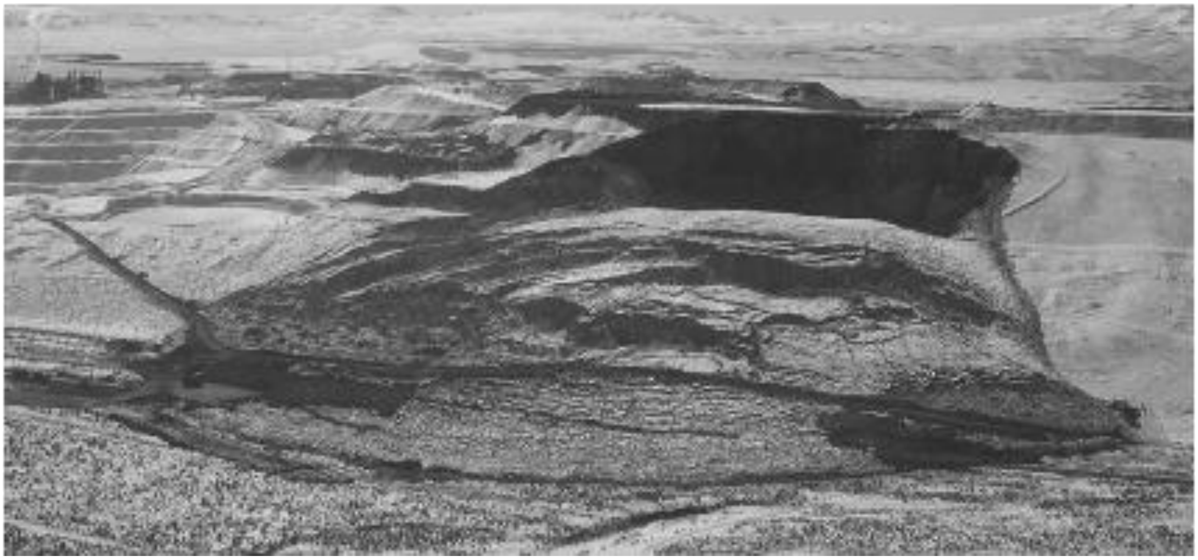

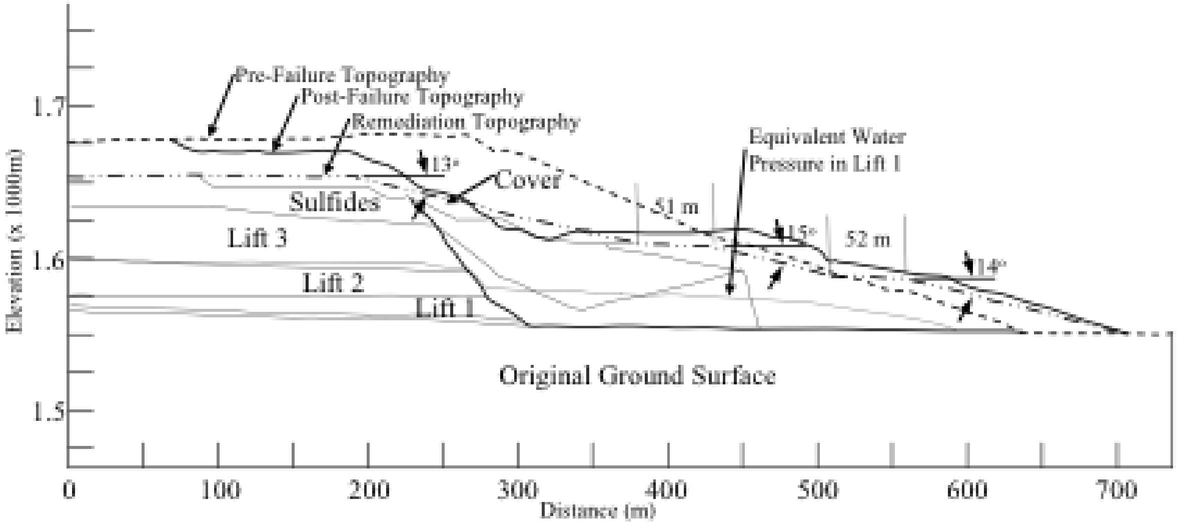
Pre-Failure Topography
Post-Failure Topography
Remediation Topography
13°
Cover
Sulfides
Lift 3
Lift 2
Lift 1
51 m
Equivalent Water
Pressure in Lift 1
15°
52 m
14°
Original Ground Surface
Elevation (x 1000m)
1.7
1.6
1.5
0
100
200
300
400
500
600
700
Distance (m)

v. Greece

vi. Turkey

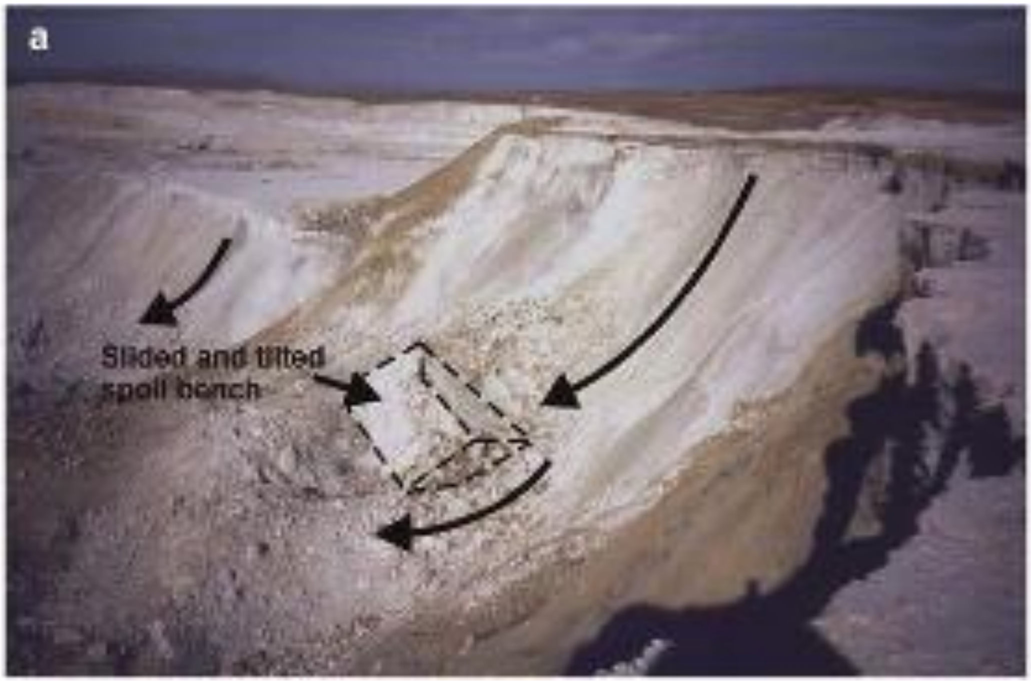
a
Slided and tilted spoil bench

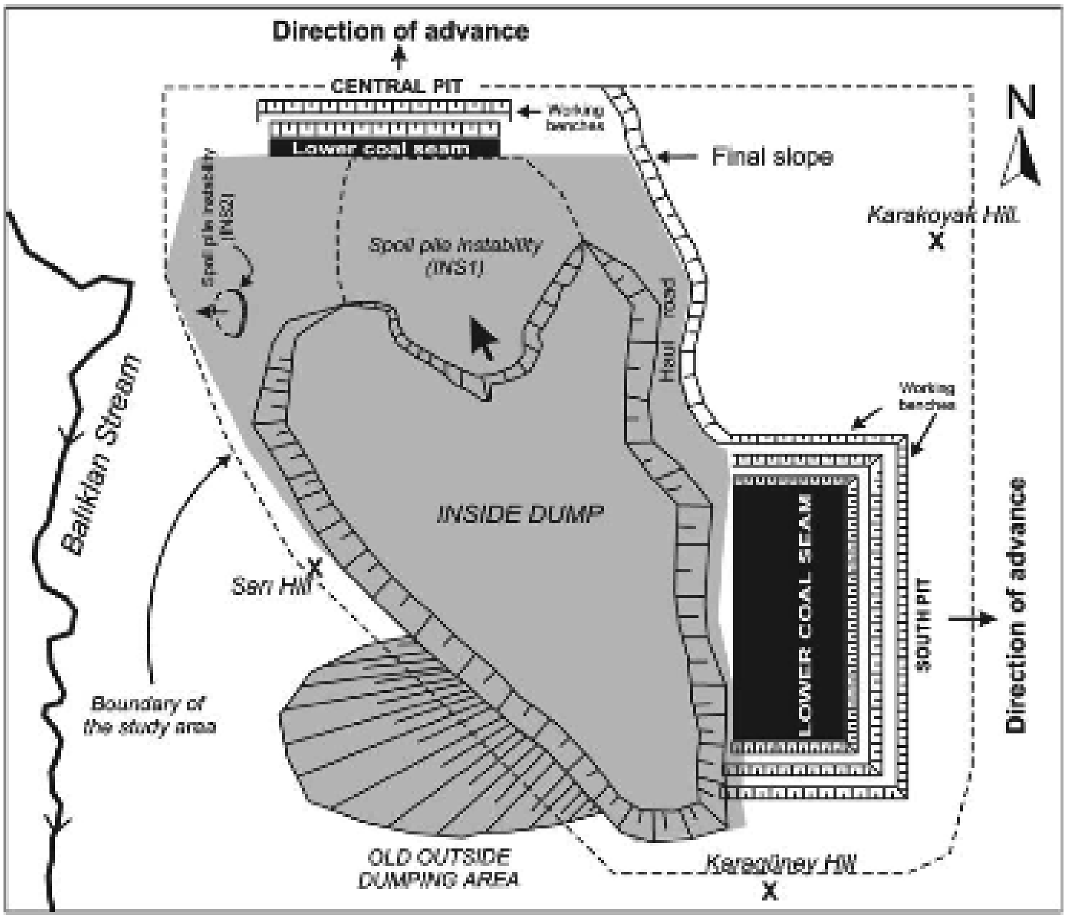
Direction of advance
CENTRAL PIT
Working benches
Lower coal seam
Final slope
N
Karakoyak Hill.
X
Spoil pile instability (INS2)
Spoil pile instability (INS1)
Haul road
Working benches
LOWER COAL SEAM
SOUTH PIT
Direction of advance
Balıklan Stream
INSIDE DUMP
Sarı Hill
Boundary of the study area
OLD OUTSIDE DUMPING AREA
Karagüney Hill
X

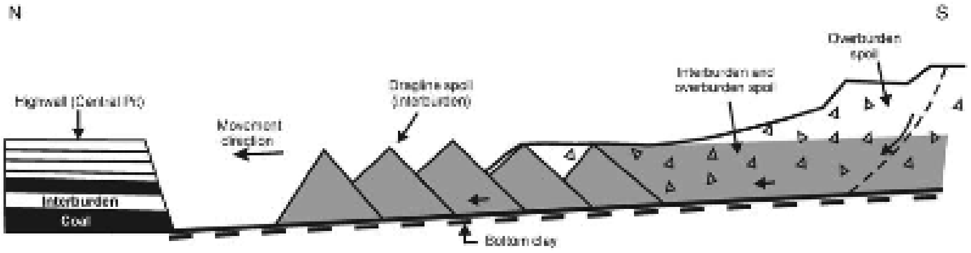
N
S
Overburden spoil
Interburden and overburden spoil
Dragline spoil (interburden)
Highwall (Central Pit)
Movement direction
Interburden
Coal
Bottom clay

APPENDIX B

The dotted curved lines above and below the best fit represent the 95% confidence limits of the regression.

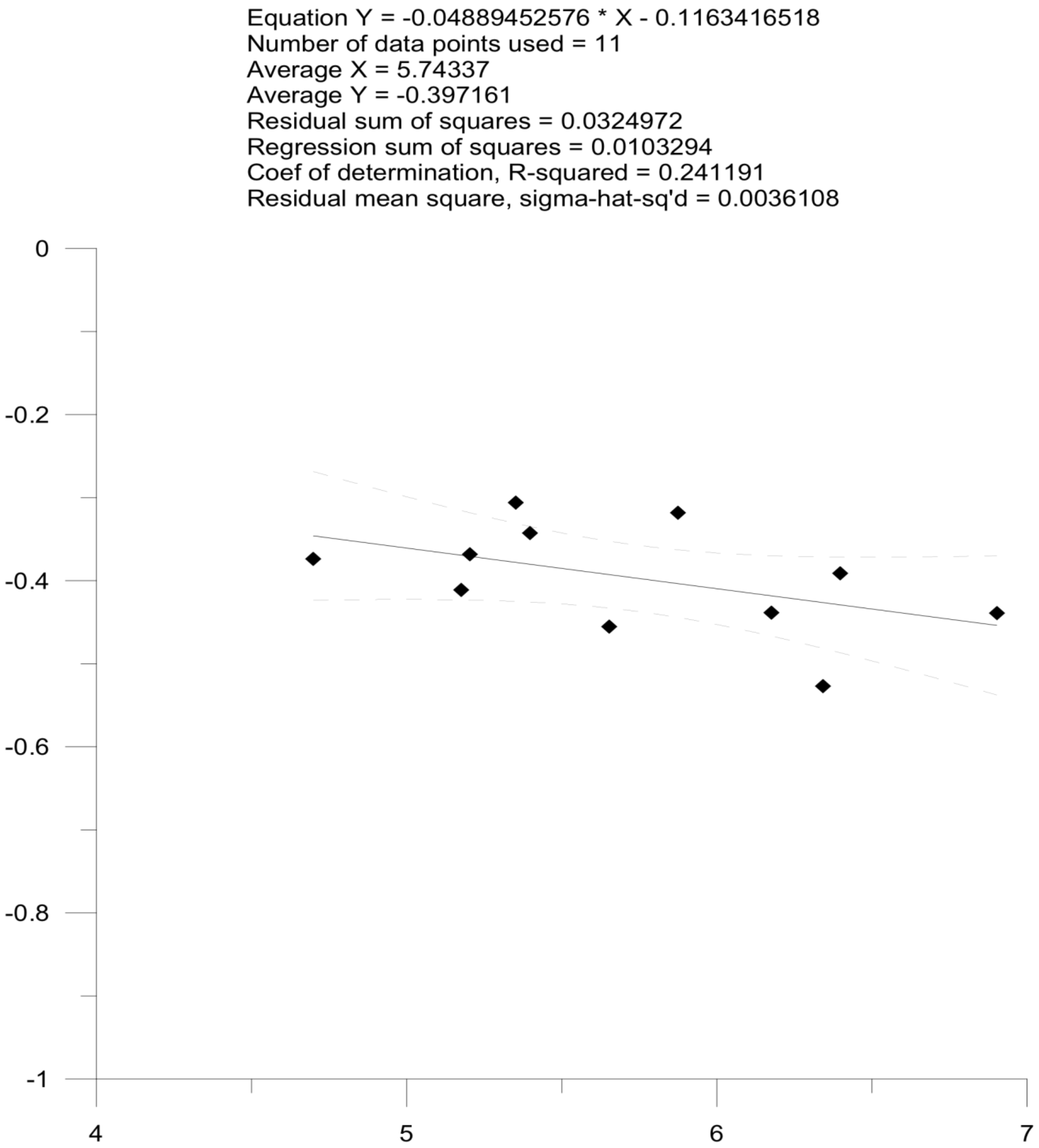

Equation Y = -0.04889452576 * X - 0.1163416518
Number of data points used = 11
Average X = 5.74337
Average Y = -0.397161
Residual sum of squares = 0.0324972
Regression sum of squares = 0.0103294
Coef of determination, R-squared = 0.241191
Residual mean square, sigma-hat-sq'd = 0.0036108

1995 Golder Data – unconfined

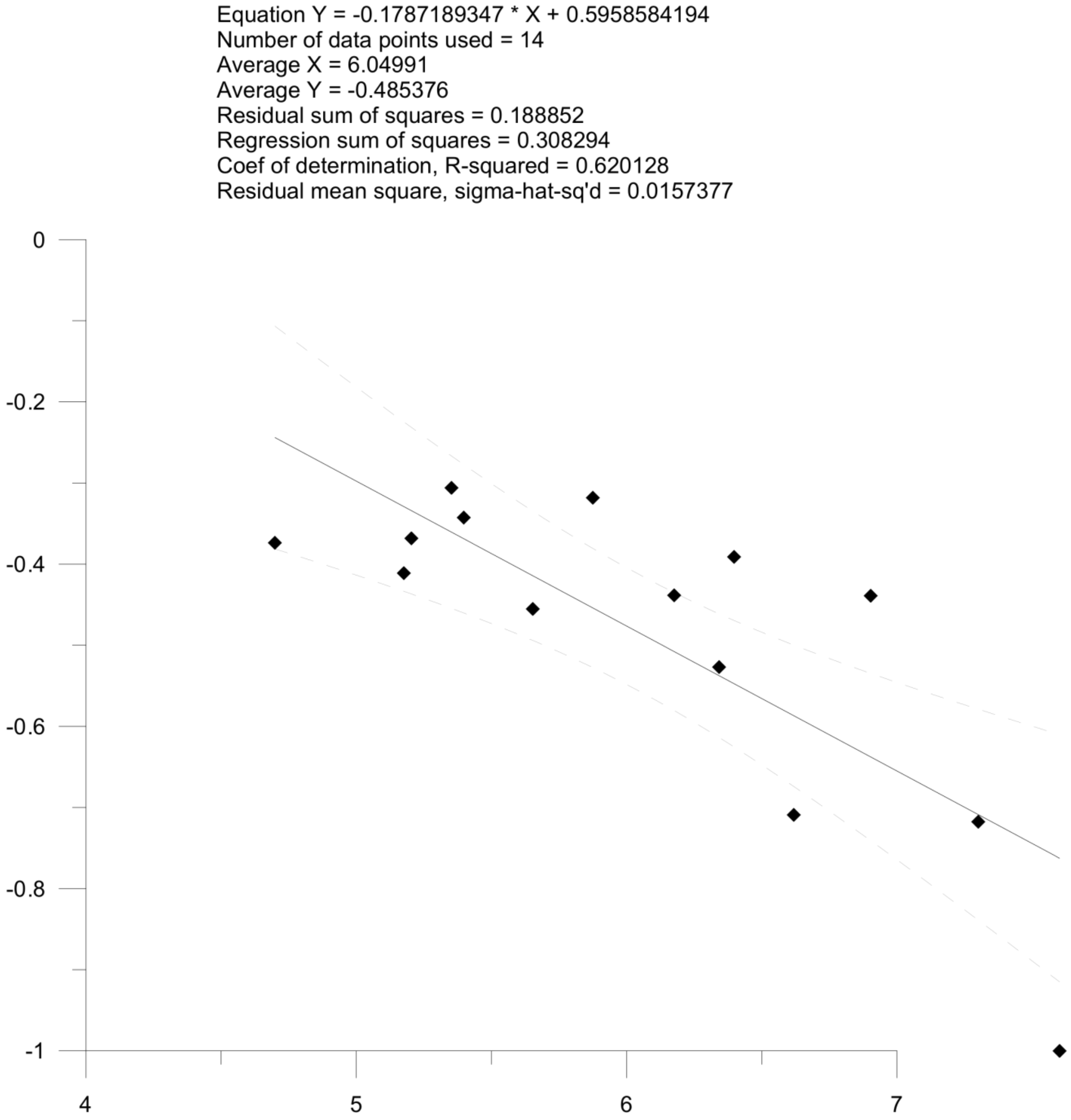

```
Equation Y = -0.1787189347 * X + 0.5958584194
Number of data points used = 14
Average X = 6.04991
Average Y = -0.485376
Residual sum of squares = 0.188852
Regression sum of squares = 0.308294
Coef of determination, R-squared = 0.620128
Residual mean square, sigma-hat-sq'd = 0.0157377
```

1995 Golder data and new data – unconfined

```
Equation Y = -0.1895364536 * X + 0.6306970867
Number of data points used = 10
Average X = 5.47225
Average Y = -0.406494
Residual sum of squares = 0.0481066
Regression sum of squares = 0.0477372
Coef of determination, R-squared = 0.498073
Residual mean square, sigma-hat-sq'd = 0.00601333
```

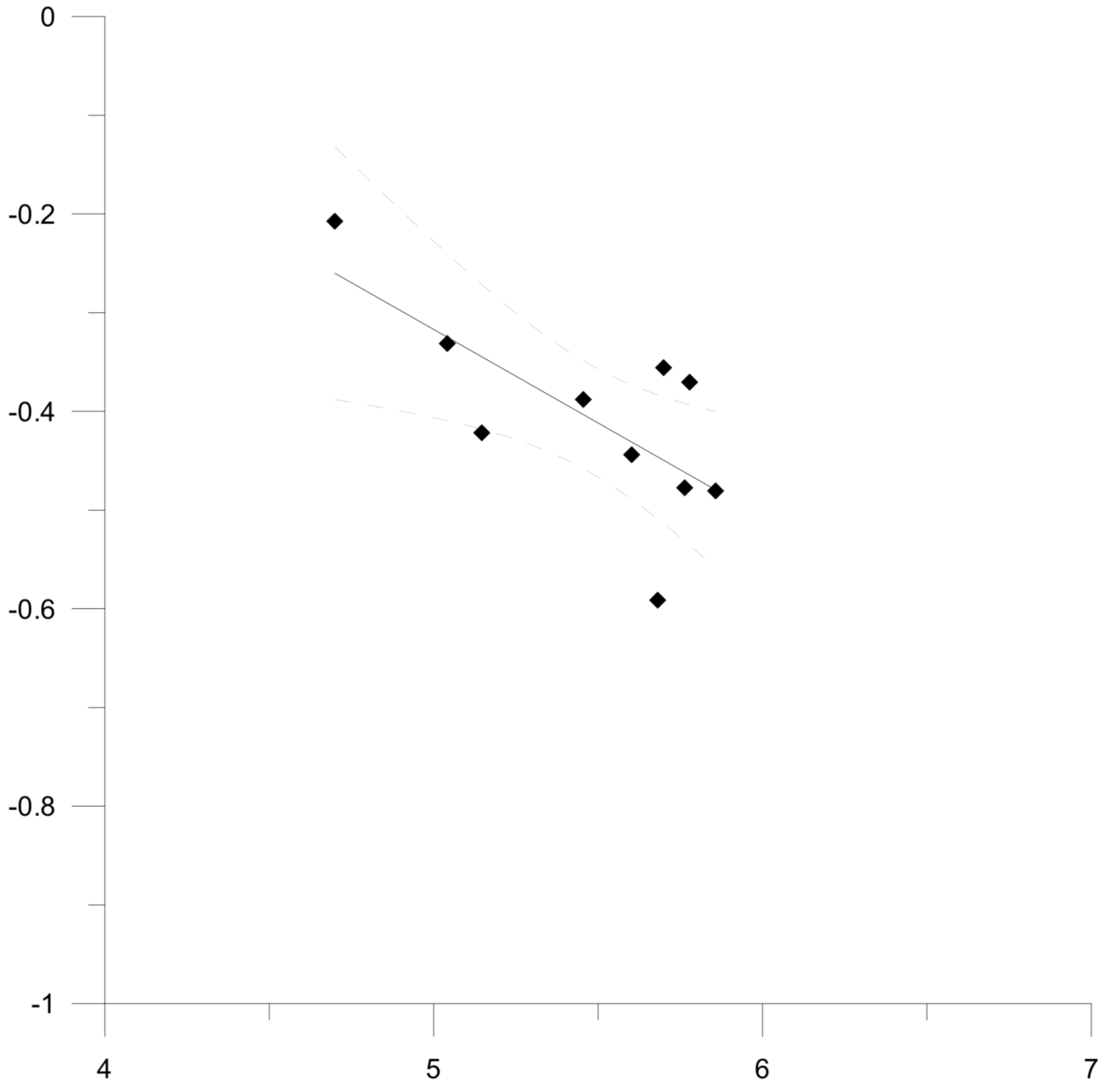

1995 Golder data – partly confined

```
Equation Y = -0.1366002406 * X + 0.3249869198
Number of data points used = 11
Average X = 5.43236
Average Y = -0.417075
Residual sum of squares = 0.0800956
Regression sum of squares = 0.0280622
Coef of determination, R-squared = 0.259456
Residual mean square, sigma-hat-sq'd = 0.00889951
```

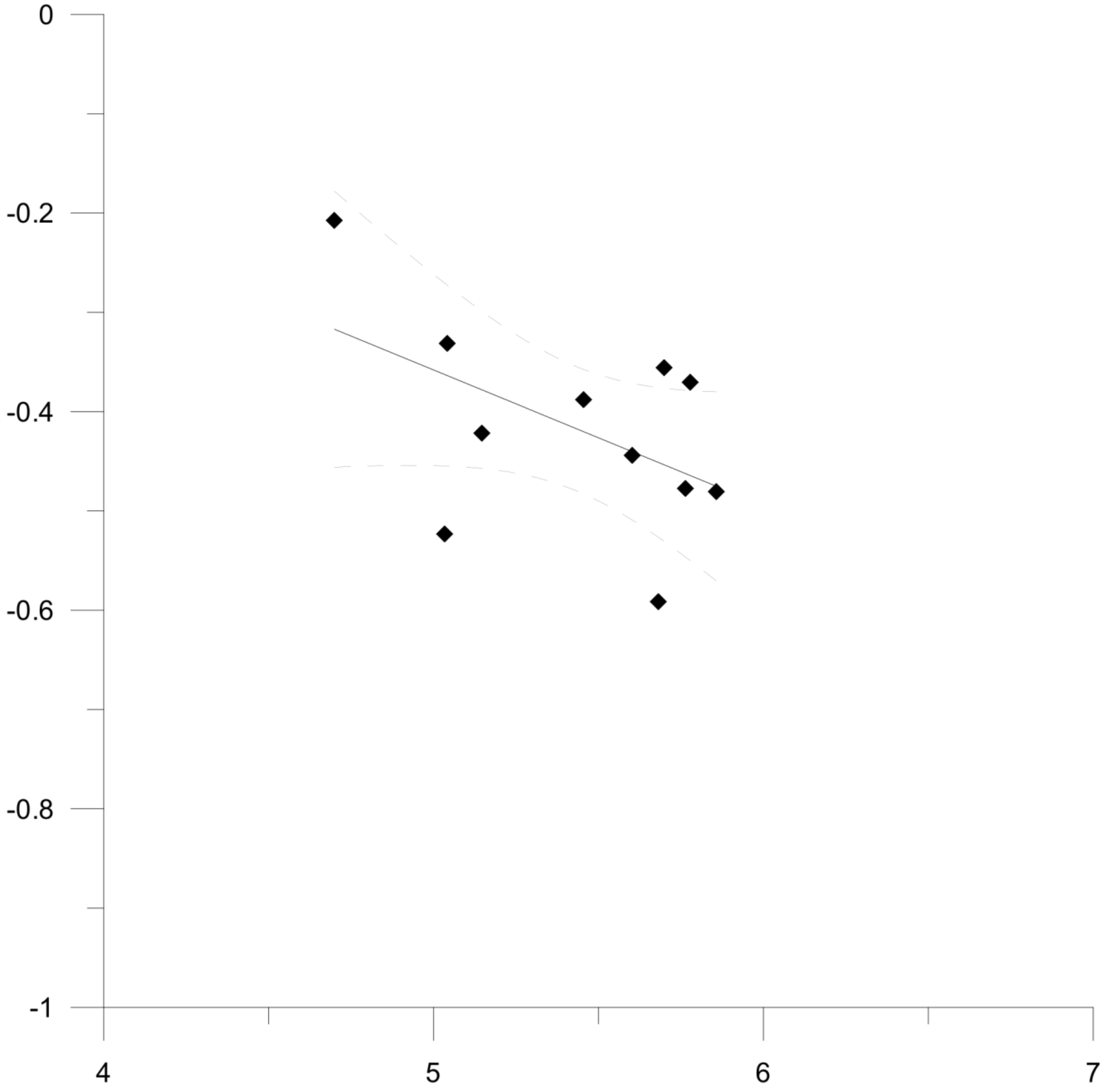

1995 Golder data and new data – partly confined

```
Equation Y = -0.1433910021 * X + 0.2497983284
Number of data points used = 18
Average X = 5.55748
Average Y = -0.547095
Residual sum of squares = 0.232214
Regression sum of squares = 0.120627
Coef of determination, R-squared = 0.341873
Residual mean square, sigma-hat-sq'd = 0.0145134
```

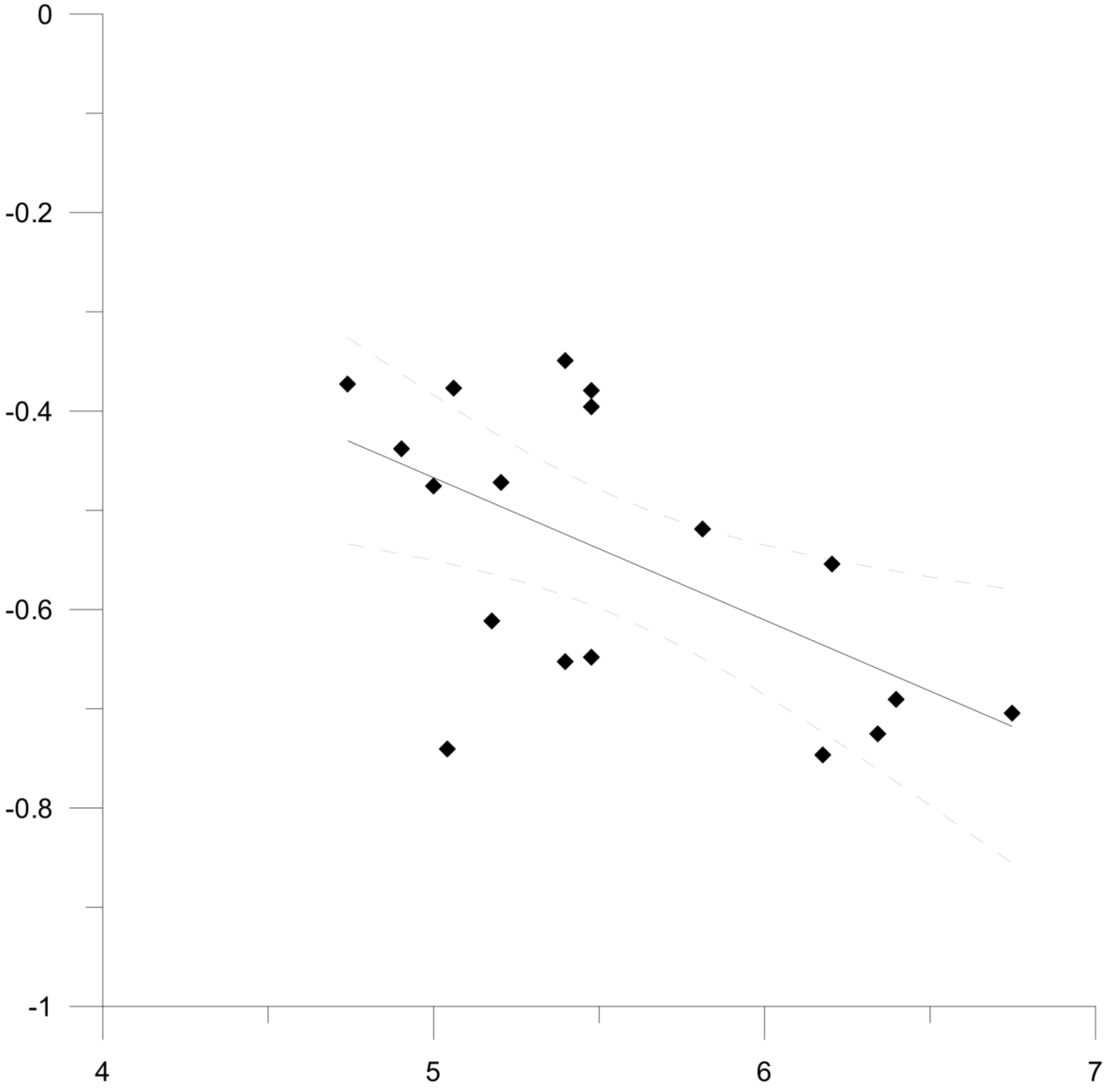

1995 Golder data – confined

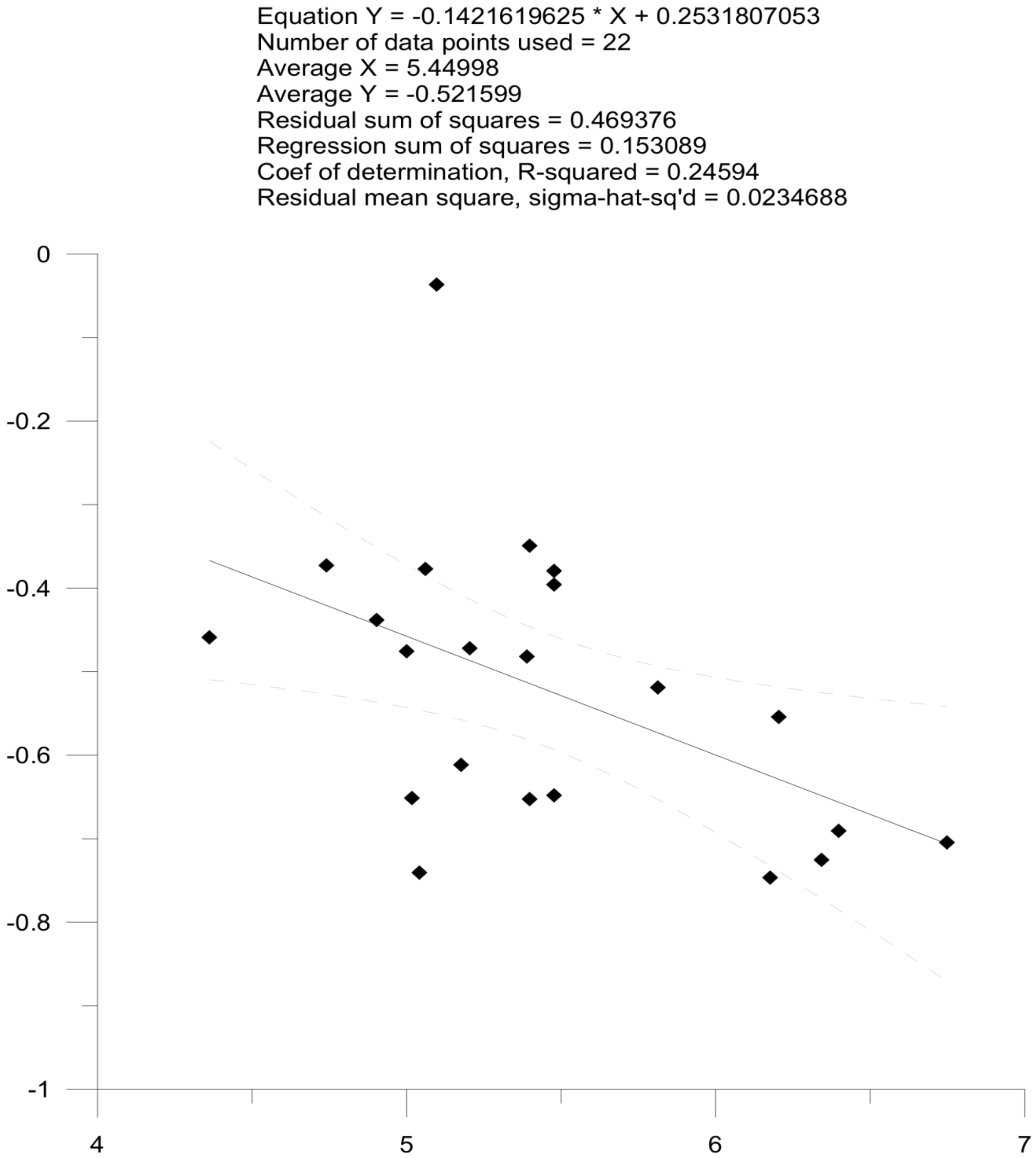

```
Equation Y = -0.1421619625 * X + 0.2531807053
Number of data points used = 22
Average X = 5.44998
Average Y = -0.521599
Residual sum of squares = 0.469376
Regression sum of squares = 0.153089
Coef of determination, R-squared = 0.24594
Residual mean square, sigma-hat-sq'd = 0.0234688
```

1995 Golder data and new data – confined

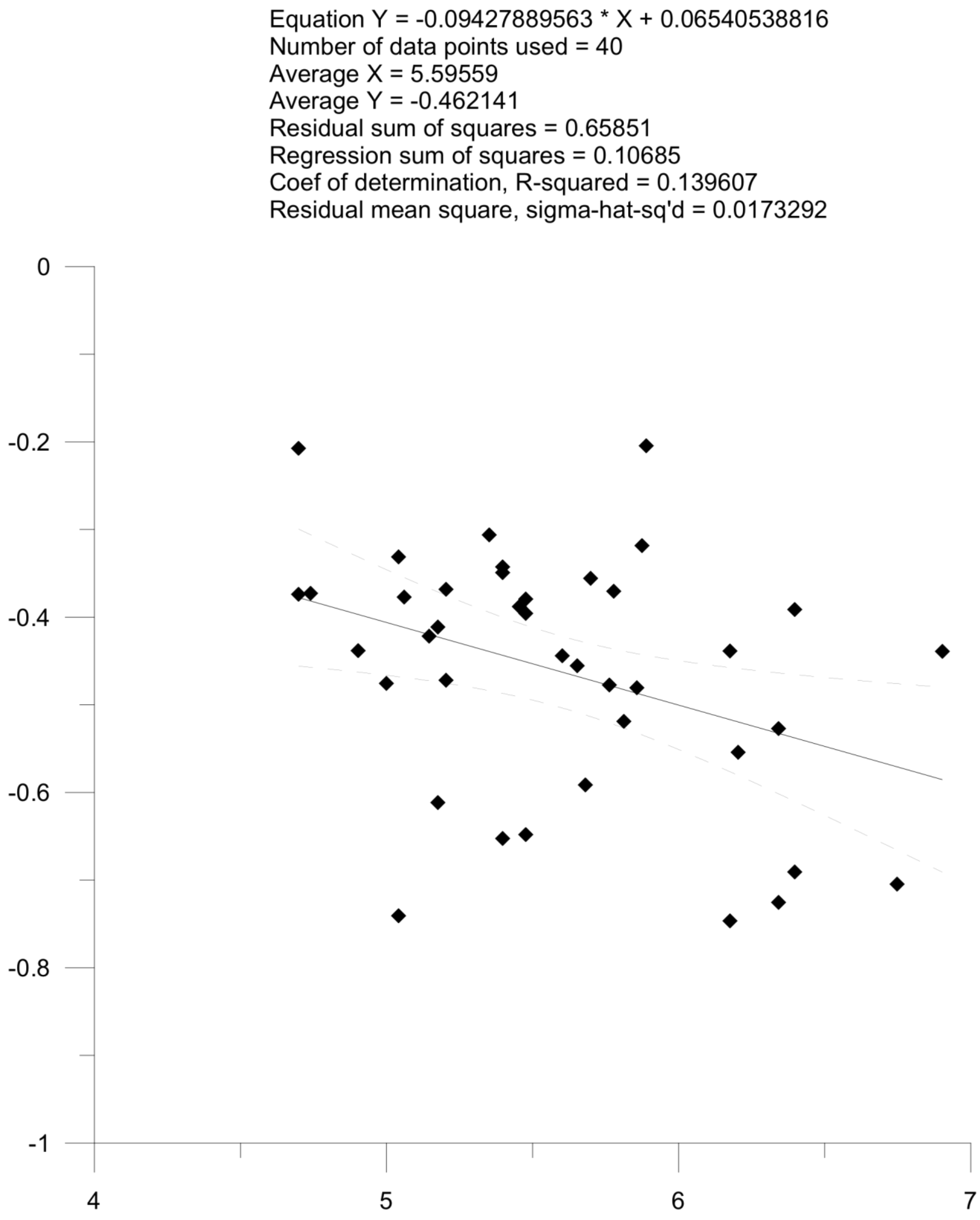

```
Equation Y = -0.09427889563 * X + 0.06540538816
Number of data points used = 40
Average X = 5.59559
Average Y = -0.462141
Residual sum of squares = 0.65851
Regression sum of squares = 0.10685
Coef of determination, R-squared = 0.139607
Residual mean square, sigma-hat-sq'd = 0.0173292
```

1995 Golder data – all cases

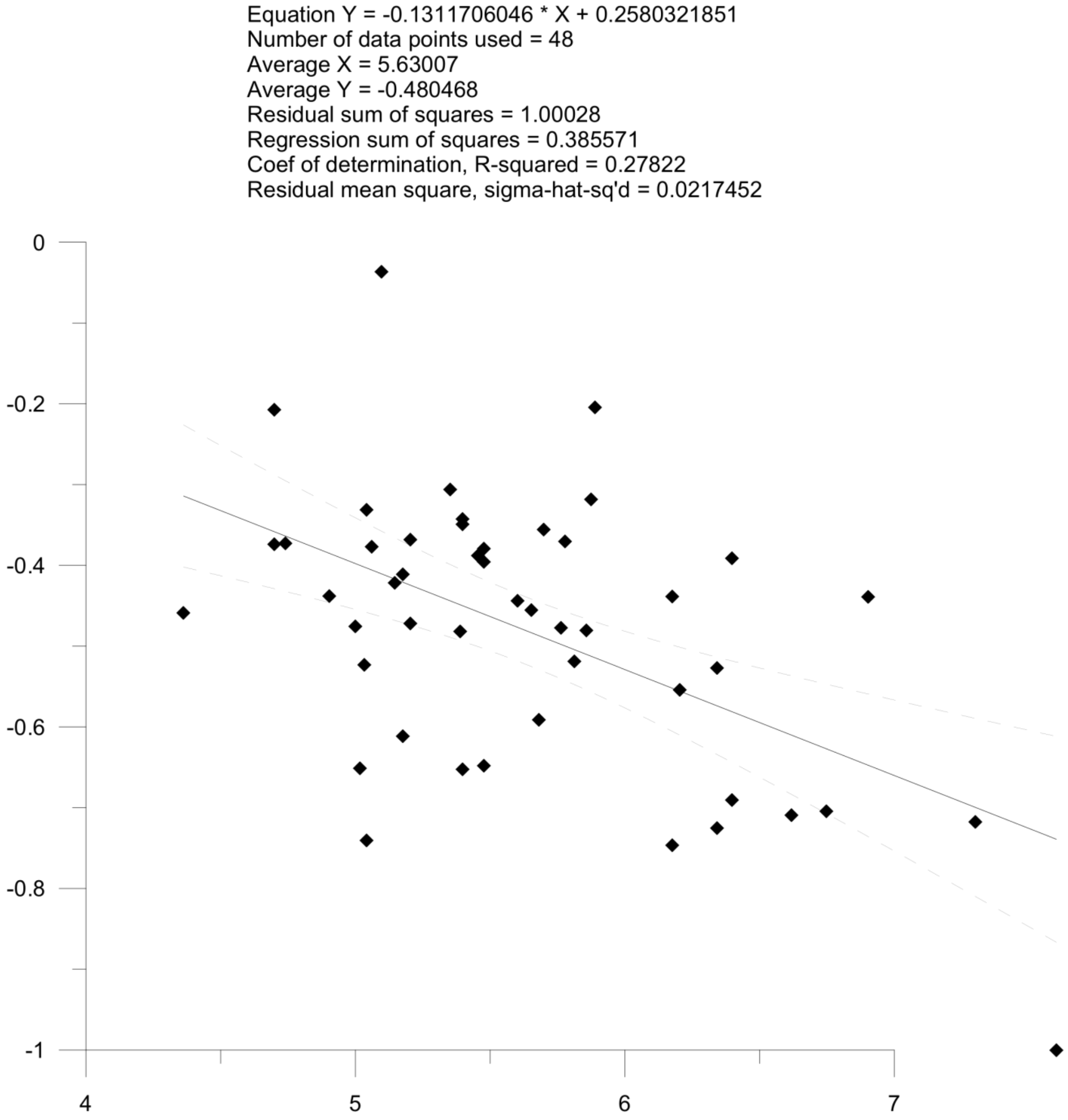

```
Equation Y = -0.1311706046 * X + 0.2580321851
Number of data points used = 48
Average X = 5.63007
Average Y = -0.480468
Residual sum of squares = 1.00028
Regression sum of squares = 0.385571
Coef of determination, R-squared = 0.27822
Residual mean square, sigma-hat-sq'd = 0.0217452
```

1995 Golder data and new data – all cases